UNIVERSIDADE DE LISBOA
FACULDADE DE CIÊNCIAS
DEPARTAMENTO DE QUÍMICA E BIOQUÍMICA


# Characterizing the regulation of the CFTR protein by the kinase GRK5 in cystic fibrosis models

Mariana Ferreira Caleiro

**Mestrado em Bioquímica e Biomedicina**

Dissertação orientada por:
Doutor Hugo Miguel Raposo Correia Botelho

2024

## Acknowledgements

Firstly, I want to thank Biosystems and Integrative Science Institute, Professor Margarida Amaral and all Cystic Fibrosis Research Lab colleagues for their help, sharing and kindness during the last year. I would like to especially thank my supervisor Hugo M. Botelho for all his support, sympathy, knowledge sharing and brainstorming, which made me feel supported and heard during the thesis.

I acknowledge the support of Rita Pacheco, Vasco Cachatra and Cristina Moiteiro from CQE/FCUL, Vukosava Torres and Helena Gaspar from the BioISI Mass Spectrometry Facility.

I would like to extend my thanks to the incredible friends who continued or began to be part of my life over the last two years, Ana Luísa, Isabelle, Maria Inês, Marta, Sházia and Violeta, whose friendship, support, advice and help were essential to face this challenge.

Finally, but not least, a huge thanks to my parents, Conceição and Luis, for all the support, and for always encouraging me to look further and pursue my goals.

All the work was supported by centre grants UIDB/04046/2020 and UIDP/04046/2020 (to BioISI) and grant NewKinCF, 2022.03453.PTDC (to Hugo M. Botelho), from FCT/MCTES and through national funds, under the projects UIDB/00100/2020, UIDP/00100/2020. Mariana Ferreira Caleiro was a recipient of a BioISI Junior BII fellowship, under the project UIDP/04046/2020 (to BioISI).

## Abstract

Cystic Fibrosis (CF) is a rare genetic disease caused by the inheritance of two alleles with pathogenic variants of the CF transmembrane conductance regulator (*CFTR*) gene. The *CFTR* gene encodes a transmembrane channel that conducts $Cl^-$ and $HCO_3^-$ across the plasma membrane (PM) of epithelial cells. Although nowadays, highly effective CFTR modulator drugs are available for people with one or two p.Phe508del-CFTR alleles – the most common CFTR variant – their high cost, and the fact that they are the only therapeutic able to stop the CF pathogenesis cascade make it necessary to develop new therapeutical options. Our group has previously identified G-protein coupled receptor kinase 5 (GRK5) as a novel regulator of p.Phe508del-CFTR. In the present work, we aimed to assess the effect of GRK5 inhibition in rescuing p.Phe508del-CFTR traffic and function and its additivity with two approved CFTR modulators, VX-661 and VX-445. To inhibit GRK5, the selective inhibitor CCG273441 was used alone and in combination with modulators.

The results allowed us to better understand GRK5-CFTR signalling pathway and how GRK5 inhibition can rescue p.Phe508del-CFTR traffic and function while confirming synergy with CFTR modulators. Once GRK5 is inhibited, the pool p.Phe508del-CFTR increases resulting in more CFTR prone to be corrected by the CFTR modulators and an increased amount of functional CFTR at the PM. In conclusion, our results show that GRK5 regulates p.Phe508del-CFTR by interfering with CFTR production and/or degradation.



**Keywords:** Cystic Fibrosis, p.Phe508del-CFTR, CFTR modulators, GRK5, membrane traffic.

## Resumo

A fibrose quística (FQ) é uma doença genética rara que afeta cerca de 160.000 pessoas em todo o mundo e cuja esperança média de vida ronda os 50 anos nos países desenvolvidos graças ao diagnóstico precoce e à disponibilidade de fármacos inovadores e eficazes. Esta doença afeta múltiplos órgãos, tais como as vias aéreas, os intestinos, o pâncreas, o fígado, e é causada pela herança de variantes patogénicas do gene do regulador de condutância transmembranar da fibrose quística (*CFTR*) em ambos os alelos. O gene *CFTR* codifica uma proteína com o mesmo nome e cuja função é conduzir iões cloreto ($Cl^-$) e bicarbonato ($HCO_3^-$) através da membrana plasmática (MP) das células epiteliais. A CFTR é um canal transmembranar composto por cinco domínios: dois domínios transmembranares (MSD1 e MSD2), dois domínios citosólicos de ligação de nucleótidos (NBD1 e NBD2) comuns entre os transportadores *ATP-binding cassete* (ABC), e um domínio regulador adicional (RD). Cada MSD é composto por 6 segmentos (TM1–TM6 e TM7–TM12) e forma o poro do canal que permite o fluxo transmembranar de $Cl^-$ e $HCO_3^-$. NBD1 e NBD2 são essenciais para a regulação da CFTR, pois a sua dimerização dependente de adenosina trifosfato (ATP) é necessária à abertura (*gating*) do canal. Por fim, o RD consiste em uma região intrinsecamente desordenada cuja fosforilação por PKA leva à dimerização dos NBD. Aquando da síntese e enrolamento da CFTR no retículo endoplasmático, ocorre co-transducionalmente uma glicosilação que origina uma proteína imatura que será sujeita ao controlo de qualidade do retículo endoplasmático (ERQC). Encontrando-se corretamente enrolada, é transportada para o complexo de Golgi onde é concluída a glicosilação e alcançada a sua forma madura, que será depois transportada para a MP onde desempenhará a sua função.

Até hoje, foram identificadas mais de 2100 variantes do gene *CFTR*, tanto patogénicas como não patogénicas. As variantes patogénicas podem comprometer o equilíbrio transepitelial de iões de diferentes formas. Atualmente, estas mutações estão agrupadas em 7 classes: Classe I inclui as mutações que prejudicam a produção de CFTR levando geralmente à degradação do mRNA (principalmente mutações nonsense); Classe II inclui mutações que resultam num enrolamento incorreto da CFTR e que levam à sua retenção pelo mecanismo de ERQC e subsequente degradação, reduzindo substancialmente o tráfego de CFTR para a membrana bem como a sua função. A p.Phe508del, a variante mais comum em indivíduos com FQ, é um exemplo de mutação de classe II; Classe III inclui as mutações que afetam o *gating* do canal; Classe IV inclui mutações que resultam na redução da condutância de $Cl^-$ e $HCO_3^-$; Classe V inclui mutações que levam à geração de mRNA aberrante por *splicing* alternativo; Classe VI inclui as mutações que resultam na destabilização da CFTR na MP, por aumento da endocitose ou diminuição da sua reciclagem de volta à MP; Classe VII inclui mutações conhecidas como irresgatáveis visto que inibem a síntese de mRNA e, consequentemente, de proteína CFTR.

Quando a CFTR não se encontra funcional na MP, a absorção de fluidos e secreção de iões fica comprometida, o que leva á perda de homeostase transepitelial que resulta na produção de muco espesso. A presença de muco espesso e mais ácido que o normal compromete o normal funcionamento dos cílios resultando na obstrução das vias aéreas e no surgimento de infeções bacterianas recorrentes, capazes de desencadear respostas inflamatórias crónicas que levam à destruição progressiva do tecido pulmonar resultando eventualmente em insuficiência respiratória. A insuficiência respiratória é a principal causa de morbidade e mortalidade entre indivíduos com FQ.

Só a partir de 2012, surgiram opções terapêuticas focadas não no controlo dos sintomas, mas sim na correção dos defeitos primários das variantes CFTR patogénicas – medicamentos chamados moduladores da CFTR. Os moduladores aprovados aumentam o enrolamento e o tráfego da CFTR (corretores) ou a abertura dos canais já presentes na MP (potenciadores). Atualmente estão aprovados pela Agência Europeia de Medicamentos (EMA) e pela *Food and Drug Administration* (FDA) dos EUA quatro moduladores da CFTR: os corretores lumacaftor (VX-809), tezacaftor (VX-661) e elexacaftor (VX-445), e o potenciador ivacaftor (VX-770). Em 2019, uma combinação de alta eficiência composta

por elexacaftor, tezacaftor e ivacaftor, conhecida comercialmente como Kaftrio, foi aprovada para uso clínico. No entanto, estes medicamentos inovadores estão disponíveis apenas para indivíduos com um ou dois alelos p.Phe508del-CFTR. Mesmo para genótipos p.Phe508del-CFTR, estes medicamentos – a única terapêutica que visa a origem da patologia – têm custo bastante elevado, tornando necessário o desenvolvimento de novas terapias para indivíduos portadores de p.Phe508del-CFTR. Por outro lado, apesar de ser a variante mais comum, é de extrema importância o desenvolvimento de opções terapêuticas para indivíduos com FQ portadores de outras variantes.

O nosso grupo identificou anteriormente a cinase 5 do receptor acoplado à proteína G (GRK5) como um novo regulador da p.Phe508del-CFTR. Nesse estudo, a regulação de p.Phe508del-CFTR pela GRK5 foi confirmada por meio de silenciamento com siRNAs e inibição com compostos inibitórios específicos. Foi observado que a inibição da GRK5 pode restaurar o tráfego de p.Phe508del-CFTR para a MP e apresenta um efeito aditivo a moduladores de CFTR usados atualmente. No entanto, a base molecular para a regulação de p.Phe508del-CFTR por meio de GRK5 é desconhecida.

As cinases do recetor acoplado à proteína G (GRK) são serina/treonina cinases conhecidas por modularem a sinalização de recetores acoplados à proteína G (GPCR), através da sua dessensibilização. Este processo canónico é comum a todas as GRK (GRK1-7) e essencial para a proteção das células e tecidos contra a exposição prolongada a ligantes bem como sustentar a resposta fisiológica contínua a estímulos. A GRK5 está também envolvida noutros processos moleculares tais como: regulação da hipertrofia cardíaca por meio da fosforilação da histona desacetilase 5 (HDAC5), redução da inflamação pela fosforilação de NF-κB p105, aumento da polimerização e agregação de α-sinucleína pela fosforilação da mesma.

Até recentemente, todos os inibidores de GRK5 disponíveis eram inespecíficos, inibindo também a GRK2. Alguns exemplos destes inibidores são o Sunitinib, um inibidor do recetor tirosina cinase aprovado pela FDA também capaz de inibir a GRK5, e o Ullrich 57, composto derivado da estrutura indolinona do Sunitinib. Os primeiros inibidores GRK5 seletivos e potentes foram desenvolvidos por Andrew D. White e pelo seu grupo, que geraram uma série de inibidores da GRK5 a partir do *scaffold* Ullrich 57. Dos inibidores gerados, os três mais seletivos e potentes foram CCG273463, CCG273441 e GRL018-21.

Posto isto, o objetivo deste trabalho foi avaliar e caracterizar o resgate do tráfego e da função da p.Phe508del-CFTR aquando da inibição da GRK5, e verificar a existência de aditividade com os moduladores de CFTR VX-661 e VX-445. Para a inibição da GRK5, foi utilizado um inibidor seletivo, CCG273441, tanto sozinho como em combinação com os moduladores referidos.

Os nossos resultados permitiram-nos entender melhor o funcionamento da via de sinalização de GRK5-CFTR e como a inibição de GRK5 é capaz de resgatar o tráfego e a função de p.Phe508del-CFTR. Foi também possível confirmar a sinergia da inibição da GRK5 com moduladores de CFTR. Uma vez inibida a GRK5, a quantidade total de p.Phe508del-CFTR nas células aumenta, havendo assim mais CFTR disponível para ser corrigida pelos moduladores e consequentemente uma quantidade aumentada de CFTR funcional no MP. Em conclusão, os nossos resultados mostram que a GRK5 regula p.Phe508del-CFTR interferindo ao nível da produção e/ou degradação de CFTR.

**Palavras-chave:** Fibrose Quística, p.Phe508del-CFTR, moduladores de CFTR, GRK5, tráfego membranar.

# Table of Contents

**Acknowledgements** ..... **II**
**Abstract** ..... **III**
**Resumo** ..... **IV**
**List of Figures** ..... **VII**
**List of Tables** ..... **VII**
**List of Abbreviations** ..... **VIII**
**1. Introduction** ..... **1**
1.1. Cystic Fibrosis ..... 1
1.1.1. General description ..... 1
1.1.2. Pathophysiology ..... 1
1.1.3. Therapeutical Options ..... 2
1.1.4. Functional Classification of CF-Causing Mutations ..... 3
1.1.5. CFTR protein – function, structure, folding, trafficking and degradation ..... 4
1.2. GRK5 in CFTR regulation ..... 5
1.2.1. GRK5 canonical and non-canonical functions ..... 6
1.2.2. GRK5 inhibitors ..... 6
**2. Objectives** ..... **7**
**3. Materials and Methods** ..... **8**
3.1. Small molecules ..... 8
3.2. Mass spectrometry ..... 8
3.3. Cell culture ..... 8
3.3. Western blot ..... 8
3.4. Halide-Sensitive Yellow Fluorescent Protein (hsYFP) quenching assay ..... 9
3.5. Statistical Analysis ..... 10
**4. Results and Discussion** ..... **10**
4.1. Validation of the CCG273463 stock ..... 10
4.2. CCG273441 effect on p.Phe508del-CFTR traffic in CFBE cell line ..... 11
4.3. CCG273441 effect on p.Phe508del-CFTR traffic in 16HBE cell line ..... 13
4.4. CCG273441 impact on p.Phe508del-CFTR function in CFBE cell line ..... 14
**5. Conclusion and Future perspectives** ..... **16**
**6. References** ..... **18**
**7. Supplementary Materials** ..... **22**

# List of Figures

Figure 1.1. Pathophysiology cascade in CF lung disease ..... 2
Figure 1.2. Classes of CFTR mutations ..... 4
Figure 1.3. CFTR structural model ..... 5
Figure 1.4. CCG273463 (9g) effect on p.Phe508del-CFTR expression and function ..... 6
Figure 4.1. CCG273463 effect on p.Phe508del-CFTR processing ..... 11
Figure 4.2. CCG273441 effect on p.Phe508del-CFTR processing ..... 12
Figure 4.3. Effect of the CCG273441, VX-661 and VX-445 combination on p.Phe508del-CFTR processing in CFBE cells ..... 13
Figure 4.4. Effect of the CCG273441, VX-661 and VX-445 combination on p.Phe508del-CFTR processing in 16HBE cells ..... 14
Figure 4.5. Effect of the CCG273441, VX-661 and VX-445 combination on p.Phe508del-CFTR channel activity ..... 15
Figure 4.6. Initial hsYFP Fluorescence ..... 16
Figure 7.1. Mass spectra of the CCG273463 stock solution. ..... 22

# List of Tables

Table 1.1. GRK5-inhibitors chemical properties ..... 7

# List of Abbreviations

| | |
|---|---|
| 16HBE | Human Bronchial Epithelial cell line |
| ABC | ATP-binding cassette |
| APS | Ammonium persulfate |
| ASL | Airway surface liquid |
| ATP | Adenosine triphosphate |
| CF | Cystic Fibrosis |
| CFBE | Cystic Fibrosis Bronchial Epithelial cells |
| CFTR | Cystic Fibrosis Transmembrane Conductance Regulator |
| $Cl^-$ | Chloride |
| DMSO | Dimethyl sulfoxide |
| DPBS | Dulbecco's phosphate buffered saline |
| EDTA | Ethylenediaminetetraacetic acid |
| EMA | European Medicines Agency |
| ER | Endoplasmic reticulum |
| ERQC | Endoplasmic reticulum quality control |
| FBS | Fetal bovine serum |
| FDA | Food and Drugs Administration |
| FIS | Forskolin-induced swelling |
| GFP | Green Fluorescent Protein |
| GPCR | G-protein coupled receptor |
| GRK | G-protein coupled receptor kinase |
| $HCO_3^-$ | Bicarbonate |
| HDAC5 | Histone deacetylase 5 |
| hsYFP | Halide-sensitive yellow fluorescence protein |
| MCC | Mucociliary clearance |
| MEM | Minimum essential medium |
| MSD1/2 | Membrane-spanning domains |

| | |
|---|---|
| NBD1/2 | Nucleotide-binding domain 1/2 |
| PCL | Periciliary fluid layer |
| PBS | Phosphate buffered saline |
| PKA | Protein Kinase A |
| PM | Plasma membrane |
| PpFEV1 | Percent predicted forced expiratory volume |
| PVDF | Polyvinylidene difluoride |
| pwCF | People with cystic fibrosis |
| RD | Regulatory domain |
| SDS | Sodium dodecyl sulfate |
| TM1-12 | Transmembrane segments |
| Tris-HCl | Tris(hydroxymethyl)aminomethane hydrochloride |
| WB | Western blot |

# 1. Introduction

## 1.1. Cystic Fibrosis

### 1.1.1. General description

Cystic Fibrosis (CF) is a monogenic autosomal recessive disease known to affect an estimated 160,000 people worldwide of which almost 50,000 live in Europe and around 40,000 in the US (Cromwell et al., 2023; Elborn, 2016; Guo et al., 2022). The frequency of CF is higher in populations of northern European descent, with the estimated incidence between 1/3000 and 1/6000 in those populations (Elborn, 2016; Scotet et al., 2020). Although the lifespan of people with CF (pwCF) is still limited, its expectancy has increased to around 50 years in several developed countries due to early diagnosis and, since the early 2010s, the availability of CFTR-targeting drugs (Elborn, 2016; Lopes-Pacheco, 2020).

CF was described in 1938 by Dorothy Anderson, who observed the destruction of the pancreas and named the disease "Cystic Fibrosis of the pancreas" (Andersen, 1938). Years later, in 1946, Anderson and Hodges described CF as an autosomal recessive disease after studying the inheritance pattern of this disease in several families. With this, they concluded that CF is caused by mutations in the two alleles of a single gene (Andersen, 1946). This gene was only identified in 1989 and named the Cystic Fibrosis Transmembrane Conductance Regulator (*CFTR*) gene (Riordan et al., 1989). The *CFTR* gene encodes a chloride- and bicarbonate-conducting transmembrane channel with the same name that allows the transepithelial balance of ions and fluid in epithelial cells (Shteinberg et al., 2021).

### 1.1.2. Pathophysiology

CF is a multi-organ disease affecting the airways, gut, pancreas, and liver, among other organs (Shteinberg et al., 2021). The absence of functional CFTR protein at the apical plasma membrane (PM) leads to transepithelial dyshomeostasis, by impairing fluid absorption and ionic secretion across epithelia (Allan et al., 2021). In the physiological state, the airway epithelium forms an interface between the external environment and the internal milieu, presenting a thin layer of fluid known as airway surface liquid (ASL) in its luminal side. ASL originates from submucosal gland secretions and transport of water and solute across the epithelium. For proper air conduction, airway maintenance is ensured by a process known as mucociliary clearance (MCC). MCC depends on the periciliary fluid layer (PCL), a thin watery layer composed of 96% water, 1% salts, 1% lipids, 1% proteins, and 1% mucus adjacent to the epithelial cell layer, that prevents epithelium dehydration and allows proper cilia beating to move up secretions (Zajac et al., 2021). CFTR-transported bicarbonate ($HCO_3^-$) is also essential to the unfolding and expansion of mucins secreted by epithelial goblet cells. When CFTR is dysfunctional at the apical PM, a highly viscous mucus accumulates at an already dehydrated ASL. Efficient ciliary beating – which otherwise drives MCC of debris and pathogens – is also compromised, resulting in airway obstruction and the opportunity for recurrent bacterial infections, triggering chronic inflammatory responses and bronchiectasis. Another $HCO_3^-$-dependent process impaired is the airway surface liquid pH regulation affecting antimicrobial peptide functions (Shteinberg et al., 2021). Repetitive cycles of mucus accumulation, bacterial infections, and neutrophilic inflammatory responses result in progressive lung tissue destruction and remodelling, and ultimately respiratory failure (Figure 1.1.) (Coverstone & Ferkol, 2021). Respiratory failure is the major cause of morbidity and mortality among pwCF with lung transplantation being the last resource at the late stages of the disease (Allan et al., 2021; Brown et al., 2017).

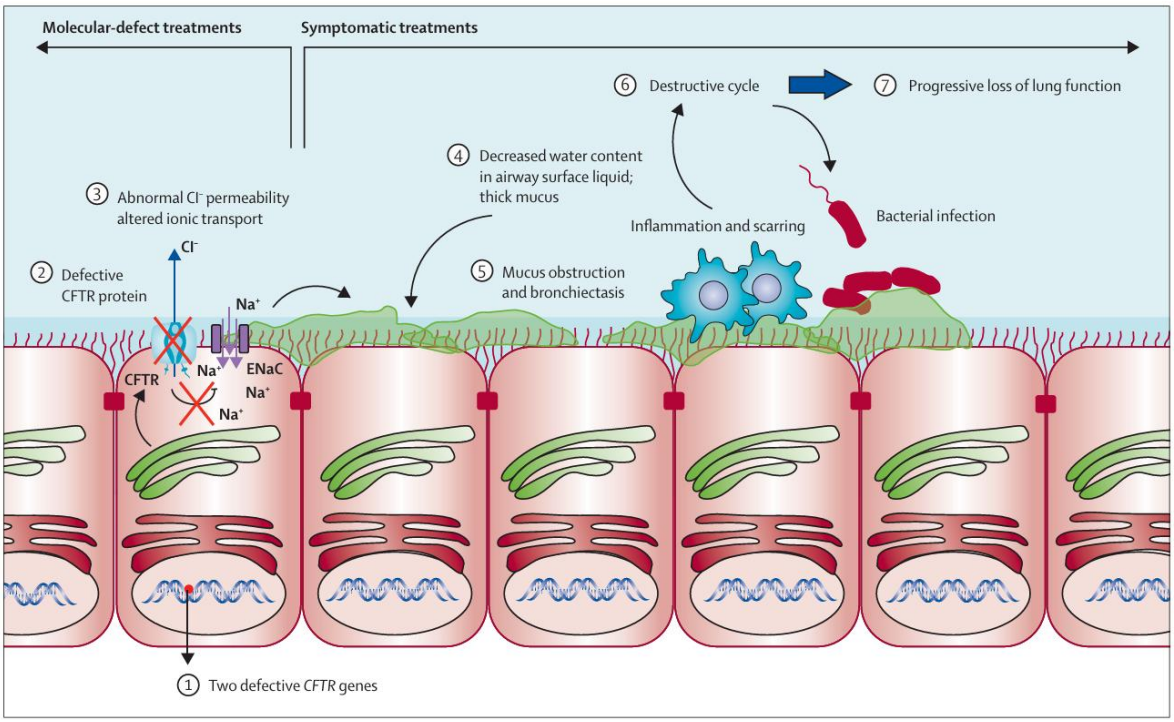


**Figure 1.1. Pathophysiology cascade in CF lung disease.** From the *CFTR* gene mutation to lung tissue destruction and loss of function. CFTR, cystic fibrosis transmembrane conductance regulator; ASL, airway surface liquid; ENaC, epithelial $Na^+$ channel. Adapted from (De Boeck & Amaral, 2016)

Moreover, CF is also characterised by pancreatic insufficiency, male infertility and comorbidities such as CF-related diabetes and CF liver disease. The cause of CF-associated pancreatic disease is epithelial damage and ductal obstruction. Pancreatic destruction can occur as result of continued duct obstruction, inflammation, fatty infiltration and fibrosis. Gastrointestinal tract complications, such as intestinal mucus obstruction and terminal ileum obstruction by thick and stick meconium result from inadequate $HCO_3^-$ secretion. CF liver disease is associated with hyperviscous biliary secretions, biliary obstruction and cirrhosis (Shteinberg et al., 2021).

### 1.1.3. Therapeutical Options

Until 2012, all treatment regimens for CF focused on managing symptoms. These symptomatic therapies include airway clearance by physical and inhaled therapy to slow lung function deterioration; improvement of pancreatic function and intestinal absorption by daily medications, such as pancreatic enzymes, fat-soluble vitamins, and high-calorie ingestion; control and eradication of bacterial infections, with the use of antibiotics and anti-inflammatories. To improve pwCF's quality of life, symptoms must be monitored by a multidisciplinary healthcare team and controlled throughout life (Brown et al., 2017; Girón Moreno et al., 2021).

Research advances have arisen from the development of preclinical cell models, such as planar cultures of polarized primary airway cells for Ussing chamber measurements (Silva et al., 2022), and implementation of cell-based high-throughput screening assays, such as halide-sensitive yellow fluorescent protein (hsYFP) quenching assay (Sondo et al., 2011) and Forskolin-induced swelling (FIS) assay of organoids (Dekkers et al., 2013; Railean et al., 2023). These advances were essential for the emergence of novel therapeutical approaches, such as drugs that directly target the primary defects of pathogenic CFTR variants, collectively known as CFTR modulators (Bacalhau et al., 2023; Lopes-Pacheco, 2020). The current modulators can increase the CFTR folding and traffic (correctors) or the

gating of channels already at the PM (potentiators) modulating mutant CFTR protein abundance and function at the apical PM (Figure 1.2.) (Lopes-Pacheco, 2020; Roda et al., 2022). Four CFTR modulator drugs are approved by the European Medicines Agency (EMA) and the US Food and Drug Administration (FDA) for people with one or two p.Phe508del-CFTR alleles: the correctors lumacaftor (VX-809), tezacaftor (VX-661) and elexacaftor (VX-445) which restore mutant CFTR protein folding and traffic, and the potentiator ivacaftor (VX-770) which enhance mutant CFTR channel gating (Allan et al., 2021). In 2019, a high-efficiency triple combination of elexacaftor, tezacaftor and ivacaftor, known as Kaftrio, was approved for clinical use. These new therapeutical drugs increased the percent predicted forced expiratory volume in 1 second ($ppFEV_1$) by around 14% during phase 3 clinical trials, which reflects lung function improvement (Heijerman et al., 2019; Middleton et al., 2019).

PwCF expectancy of life has increased from early childhood in the 1960s to around 40-50 years nowadays in several developed countries. However, pwCF continues to be exposed to clinical, psychosocial and economic burdens (Lopes-Pacheco, 2020). Although around 90% of pwCF can benefit from CFTR modulators, many cannot access them due to their extremely high cost (hundreds of thousands of dollars per year) for health systems and the requirement for lifetime usage. Thus, there is still a need to increase the number of therapeutic options for these individuals (Guo et al., 2022). The remaining CF population is not eligible for these drugs, mostly because they bear variants that lead to little or no CFTR protein expression. In this way, there's also a need to develop new therapeutical strategies for pwCF carrying these rarer mutations (Allan et al., 2021; Fajac & Sermet, 2021).

### 1.1.4. Functional Classification of CF-Causing Mutations

More than 2100 CFTR variants have been identified and consist of missense, frameshift, splicing, and nonsense mutations; large and in-frame deletions or insertions; promoter mutations; and variants presumed to be non-pathological (De Boeck & Amaral, 2016). Although most of them are assumed to cause CF by resulting in impaired $Cl^-$ and $HCO_3^-$ transepithelial balance, the impairment can occur by different mechanisms depending on the mutation, making it necessary to classify the various CF-causing mutations (Farinha & Callebaut, 2022).

The classification of CF-causing mutations was first established according to their molecular defects (functional classes) and then according to the therapeutic strategies to be used, known as theratypes (Farinha & Callebaut, 2022). Nowadays, CF-causing mutations are grouped into 7 classes (Figure 1.2.): Class I mutations (mostly nonsense mutations) impair CFTR production, often leading to mRNA degradation by nonsense-mediated decay; Class II mutations (e.g. p.Phe508del, the most common CFTR mutation present in 85% of pwCF) lead to protein misfolding, retention by the endoplasmic reticulum (ER) quality control (ERQC) mechanism, and subsequent premature degradation, which results in impaired CFTR trafficking and severely reduced function; Class III mutations affect CFTR channel gating; Class IV mutations impair the CFTR channel conductance of $Cl^-$ and $HCO_3^-$, resulting in a substantial decrease; Class V mutations result in the major reduction of normal CFTR levels, due to the generation of aberrant mRNA by alternative splicing; Class VI mutations lead to CFTR destabilization at the PM, which can occur due to increased endocytosis or decreased CFTR recycling back to the PM; Class VII mutations, known as unrescuable mutations due to inhibition of mRNA synthesis, cannot be pharmacologically rescued by the drugs currently available (De Boeck & Amaral, 2016). Classes I, II, III and VII mutations are normally related to classical CF, while class IV, V and VI mutations result in milder (known as atypical) forms of CF (Amaral, 2015; De Boeck & Amaral, 2016).

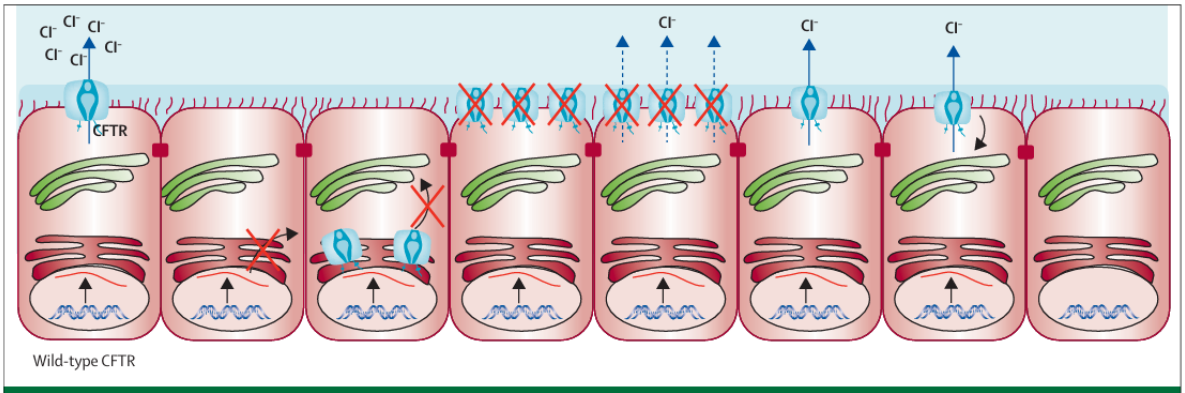


| | Class I | Class II | Class III | Class IV | Class V | Class VI | Class VII |
|---|---|---|---|---|---|---|---|
| CFTR defect | No protein | No traffic | Impaired gating | Decreased conductance | Less protein | Less stable | No mRNA |
| Mutation examples | GLy542X, Trp1282X | Phe508del, Asn1303Lys, Ala561Glu | Gly551Asp, Ser549Arg, Gly1349Asp | Arg117His, Arg334Trp, Ala455Glu | Ala455Glu, 3272-26A→G, 3849+10 kg C→T | c. 120del23, rPhe508del | dele2,3(21 kb), 1717-1G→A |
| Corrective therapy | Rescue synthesis | Rescue traffic | Restore channel activity | Restore channel activity | Correct splicing | Promote stability | Unrescuable |
| Drug (approved) | Read-through compounds (no) | Correctors (yes) | Potentiators (yes) | Potentiators (no) | Antisense oligonucleotides, correctors, potentiators? (no) | Stabilisers (no) | Bypass therapies (no) |

**Figure 1.2. Classes of CFTR mutations.** Examples of mutations, therapeutical strategies and approved drugs (if applicable) for each class are described. CFTR, cystic fibrosis transmembrane conductance regulator; rPhe508del, rescued p.Phe508del. Adapted from (De Boeck & Amaral, 2016).

Developing mutant-specific combinatorial therapies relies on the comprehensive knowledge of possible binding sites and mechanisms of action of modulators alone and in combination since many mutations result in multiple defects, being considered in multiple classes (*e.g.* p.Phe508del results in class II, III and VI defects) (Amaral, 2015; Farinha & Callebaut, 2022).

### 1.1.5. CFTR protein – function, structure, folding, trafficking and degradation

The *CFTR* gene is located on the long arm of chromosome 7 and consists of 27 exons spanning 189.36 kb (Parisi et al., 2022; Tsui & Dorfman, 2013). When transcribed, this gene produces a cAMP-regulated transmembrane glycoprotein with 1,480 amino acids, that belongs to the ATP-binding cassette (ABC) transporter superfamily (Hwang et al., 2018). The CFTR protein contains five domains: two membrane-spanning domains (MSD1 and MSD2), two cytosolic nucleotide-binding domains (NBD1 and NBD2) common among ABC transporters, plus an additional regulatory domain (RD). Each MSD is composed of 6 transmembrane segments (TM1–TM6 and TM7–TM12) and forms the channel pore that allows the $Cl^-$ and $HCO_3^-$ flow across the PM. NBD1 and NBD2 bind and hydrolyse adenosine triphosphate (ATP), which is essential for channel gating (*i.e.* opening) regulation. RD consists of an intrinsically disordered region whose phosphorylation by protein kinase A (PKA) drives NBD dimerization and channel gating (Farinha & Canato, 2017; Liu et al., 2017; Moran, 2017).

CFTR biogenesis involves the co-translational core-glycosylation, insertion of all 12 TMs into the ER membrane and folding of all domains. Although folding is almost completed during CFTR synthesis, post-translational changes mainly in the MSD1 and MSD2 lead to the formation of two transmembrane segments subgroups organized around the channel pore: TM1-2, 9-12 and TM3-6, 7-8. Both co- and post-translational mechanisms contribute to acquiring compactly folded domains and

assemble these domains to produce a fully folded structure (Figure 1.3.) (Bose et al., 2020; Farinha & Canato, 2017).

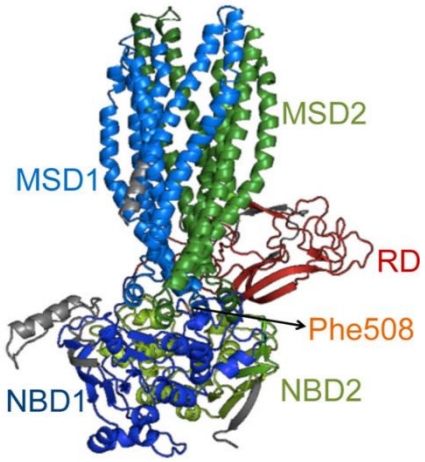


**Figure 1.3. CFTR structural model.** Intramolecular interactions between the CFTR domains are essential to achieve a compact structure. Phe508, the more commonly mutated amino acid, is marked in the figure. Adapted from (Farinha & Canato, 2017)

The ERQC is the mechanism that controls CFTR folding efficiency allowing immature folded CFTR (~145 kDa) to exit the ER, be fully glycosylated at the Golgi complex and reach its mature form (~170 kDa), get to the post-Golgi compartments and ultimately be delivered to the PM (Amaral, 2005; Farinha & Canato, 2017). CFTR levels at the PM result from a balance between trafficking, endocytosis, and recycling. For stability regulation, CFTR structure is continuously assessed by peripheral quality control mechanisms. All these regulation processes are essential to the fine modulation of $Cl^-$ and $HCO_3^-$ secretion and epithelial surface hydration (Farinha & Callebaut, 2022; Farinha & Canato, 2017).

Contrarily, unfolded and misfolded proteins, such as p.Phe508del-CFTR, are retained in the ER and targeted to degradation by the ubiquitin-proteasome pathway. The p.Phe508del variant, located in NBD1 (Figure 1.3.), was reported to delay the folding kinetics of this domain, resulting in a conformational defected CFTR. This defect results in CFTR folding impairment and increased protein degradation rate due to compromised domain-domain interactions and instability (Capurro et al., 2021; Farinha & Canato, 2017). Even when pharmacologically rescued, p.Phe508del-CFTR is unstable at the PM being rapidly endocytosed for lysosomal degradation (Meng et al., 2017; Moniz et al., 2013).

## 1.2. GRK5 in CFTR regulation

A study previously developed by our group (Amaral et al., 2023), identified G-protein coupled receptor kinase 5 (GRK5) as a novel p.Phe508del-CFTR regulator. The GRK5 regulation of p.Phe508del-CFTR was confirmed through silencing with siRNAs and inhibition with GRK5-specific inhibitory compounds. It was observed that GRK5 inhibition can restore p.Phe508del-CFTR trafficking to the PM and presents an additive effect to currently used CFTR modulators (Figure 1.4.). The molecular basis for the regulation of p.Phe508del-CFTR through GRK5 is currently unknown.

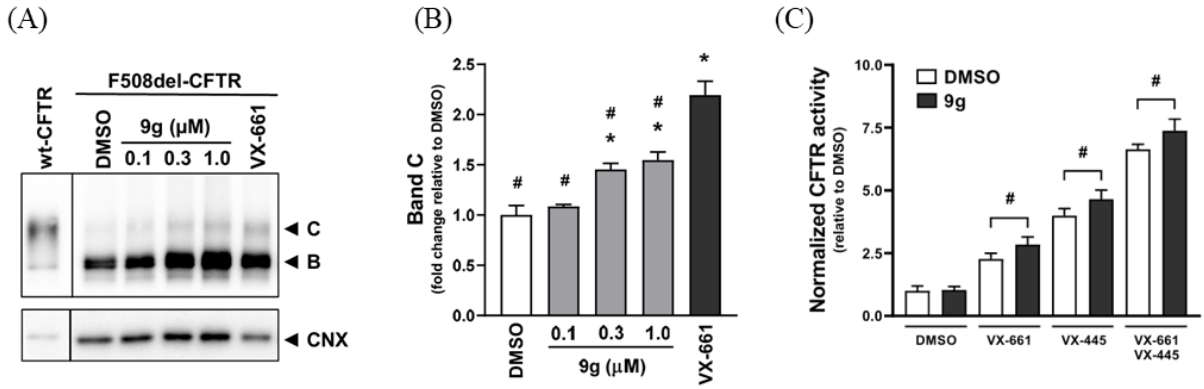


**Figure 1.4. CCG273463 (9g) effect on p.Phe508del-CFTR expression and function.** Detection (A) and quantification (B) of p.Phe508del-CFTR (C and B bands) and calnexin (CNX) expression in CFBE cell lysates through western blotting. *, statistical significance from DMSO; #, statistical significance from VX-661 ($p>0.05$, one-way ANOVA followed by Dunnett's post-hoc test, n=3). (C) p.Phe508del-CFTR channel activity assessed through hsYFP quenching assay. #, $p<0.05$, double-tailed unpaired t-test, n=4. All plot values are mean ± SD. Adapted from (Amaral et al., 2023).

### 1.2.1. GRK5 canonical and non-canonical functions

G-protein coupled receptor (GPCR) kinases, or GRKs, are serine/threonine kinases known to act as GPCR signaling modulators, involved in GPCR desensitization. Based on their sequence homology, the seven GRK members are divided into three subgroups: GRK1 and GRK7 belong to the rhodopsin kinase or visual GRK subfamily, GRK2 and GRK3 to the β-adrenergic receptor kinases subfamily, and GRK4, 5, and 6 to the GRK4 subfamily. The canonical process of GPCR desensitization, common among all GRKs, is essential for cell/tissue protection against prolonged harmful exposure to ligands and to sustain continued physiological responsiveness to stimuli. The GPCR desensitization is induced by GRK-associated phosphorylation of serine or threonine residues within an aspartate or glutamate context within the receptor's intracellular loops or in the carboxyl-terminus (C-terminus) of the activated GPCR. GPCR phosphorylation diminishes subsequent G-protein association and allows the stable association of β-arrestin to the activated receptor. This GPCR-β-arrestin association inhibits G-protein association, allows GRCP internalization and increases its interaction with endocytic components (*e.g.* clathrin). Once internalized, the receptor can be recycled to the PM or targeted for lysosomal degradation, depending on whether the cell surface receptor stimulation is moderate or excessive, respectively. Thus, the GPCR desensitization process is a signal modulation event rather than a signal termination event (Hendrickx et al., 2018).

Besides this canonical process, GRK5 also presents non-canonical functions by phosphorylating other substrates. GRK5 regulates cardiac hypertrophy through histone deacetylase 5 (HDAC5) phosphorylation, leading to HDAC5 nuclear export and subsequent transcription of several cardiac hypertrophy-associated genes. This kinase can also phosphorylate NF-κB p105, which reduces inflammation. In addition, GRK5 has been associated with Alzheimer's disease due to its ability to phosphorylate α-synuclein, tubulin and tau protein, and increase α-synuclein polymerization and aggregation (Hendrickx et al., 2018; Pfleger et al., 2019).

### 1.2.2. GRK5 inhibitors

Until recently, available GRK5 inhibitors also targeted GRK2. Some examples are Sunitinib, an FDA-approved receptor tyrosine kinase inhibitor, and Ullrich 57, a derivative from an indolinone scaffold of Sunitinib. The first selective and potent GRK5 inhibitors were developed by Andrew D.

White and his group (Chen et al., 2024; Rowlands et al., 2021), who generated several GRK5 inhibitors using the Ullrich 57 scaffold. The most highly selective and potent were CCG273463, CCG273441 and GRL018-21 (Table 1.1.) (Chen et al., 2024; Rowlands et al., 2021).

**Table 1.1. GRK5-inhibitors chemical properties.** Chemical structure, molecular weight, $IC_{50}$ values and selectivity of Sunitinib, Ullrich 57, CCG273441, CCG273463 and GRL018-21.

| Name | Structure | MW (g/mol) | GRK5 $IC_{50}$ (μM ± SD) | GRK2 $IC_{50}$ (μM ± SD) | Selectivity (GRK2 $IC_{50}$/ GRK5 $IC_{50}$) |
|---|---|---|---|---|---|
| CCG273441 | 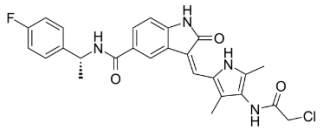 | 494.95 | 0.0038 ± 0.001 | 4.8 ± 3 | 1300 |
| CCG273463 | 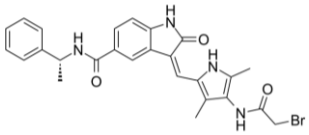 | 521.41 | 0.0086 ± 0.003 | 12 ± 20 | 1400 |
| GRL018-21 | 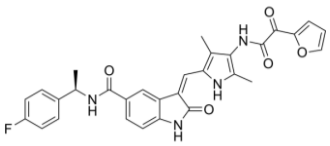 | 540.54 | 0.01 ± 0.008 | >1000 | >100,000 |
| Ullrich 57 | 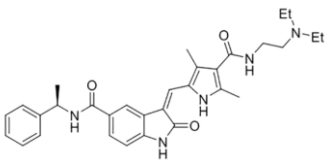 | 527.29 | 0.015 ± 0.02 | 44 ± 18 | 74 |
| Sunitinib | 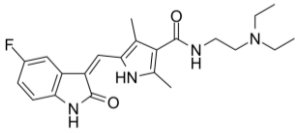 | 398.47 | 0.83 ± 0.7 | 130 ± 200 | 150 |

## 2. Objectives

This work aimed to characterize the rescue of p.Phe508del-CFTR traffic and function upon inhibition of GRK5 and its additivity with CFTR modulators, to contribute to the elucidation of the underlying signaling pathway. To this end, the following tasks were carried out:

1. Determine mature and immature p.Phe508del-CFTR protein levels in CFBE cells treated with the GRK5 inhibitor CCG273441 alone and in addition with modulators.
2. Test additivity in the endogenously expressing 16HBE bronchial epithelial cell line by combining CCG273441 with modulators.
3. Investigate the effect of CCG273441 combined with modulators on p.Phe508del-CFTR function in CFBE cells.

# 3. Materials and Methods

## 3.1. Small molecules

For the development of this work, several compounds were used, namely CFTR modulators (VX-661 and VX-445) obtained from Selleckchem, GRK5 inhibitors CCG273441 and CCG27463. CCG273441 was obtained from MedChemExpress, while CCG27463 was obtained through synthesis by Vasco Cachatra and Cristina Moiteiro, CQE/FCUL, as published (Rowlands et al., 2021).

## 3.2. Mass spectrometry

Mass spectrometry analysis was performed using a The Bruker Imapct II UHR–QqTOF (Bruker Daltonics) instrument with electrospray ionization (ESI) in positive ionization modes at the BioISI Mass Spectrometry Facility. The capillary voltage was set at 4500V, the nebulizer was set to 0.4bar, the drying gas flow rate was 5.0L/min and the drying temperature of 200 °C. The acquisition was performed in the positive ionization mode at a spectra rate of 1 Hz, in the mass range of 50 to 1500m/z. The collision energy was set to 10eV, transfer time was 70ms. The spectra were externally calibrated by infusion of the 1µM sodium formate-acetate adducts across the mass range (infusion flow 180µL/h). Calibration of MS files was performed using Compass Data Analysis 6.3 (Bruker, Daltonics) in high precision calibration mode (HPC) giving an error of <1ppm and standard deviation of < 0.2ppm.

## 3.3. Cell culture

CF Bronchial Epithelial cells (CFBE) stably expressing p.Phe508del-CFTR were cultured in Minimum Essential Medium (MEM) (Corning, #10-010-CV) containing 10% (v/v) fetal bovine serum (FBS) (Gibco, #A52567-01) and supplemented with 2µg/ml puromycin for CFTR selection. This immortalized cell line generated from a CF individual homozygous for p.Phe508del – but undetectable CFTR expression – has been used to study CFTR function and response to small molecules (Gottschalk et al., 2016).

Human Bronchial Epithelial cells (16HBE) expressing p.Phe508del-CFTR were cultured in MEM containing 10% (v/v) FBS. This cell line is derived from a Heart-lung transplant patient, expressing endogenous CFTR. (Van Den Bossche et al., 2023)

CFBE Phe508del-CFTR stably expressing halide-sensitive yellow fluorescent protein (hsYFP) were cultured in MEM containing 10% FBS and supplemented with 2µg/ml puromycin for selection.

All cell lines were thawed by adding the cryovial cellular content to complete media, followed by centrifugation at 200g for 5 min. Then, the supernatant was discarded, and the cells were resuspended in MEM containing 10% FBS and 2µg/ml puromycin and placed into a 6 cm cell culture dish.

All cell lines were cultured in a humid atmosphere with 5% $CO_2$ at 37°C. As adherent cells, when confluent cells were washed twice with Dulbecco's Phosphate Buffered Saline (DPBS) (Gibco, #14190136) and detached from 6 or 10 cm dishes with 0.05% trypsin/0.53mM EDTA ((Corning, #25-051-CI). Subsequently, MEM containing 10% FBS and 2µg/ml puromycin was added and cells were mechanically disaggregated and subcultured into new dishes.

## 3.3. Western blot

Western blotting (WB) is a biochemical technique that allows the identification and quantification of specific proteins in complex samples, such as cell lysates. To obtain the cell lysates, p.Phe508del-CFTR CFBE or 16HBE cells were seeded in 24-well plates (CFBE: 110 000 cells/well;

16HBE: 200 000 cells/well) in MEM supplemented with 10% (v/v) FBS. 24h later CCG273441 was added (75nM, 100nM, 300nM, 500nM, 750nM and 1000nM) in MEM containing 1% FBS with and without the VX-445 and VX-661 modulator combination (3μM and 5μM, respectively). 16HBE cells were only incubated with the CCG273441 concentrations in combination with modulators. Wells with VX-661 and VX-445, and vehicle (0.05% DMSO) were used as controls. Protein extraction was performed after 24h and 48h incubation. The media of CFBE cells treated for 48h was replaced after 24h. Then, cells were washed with PBS and extraction buffer was added. The extraction buffer used contained 31.25 mM Tris HCl (Sigma-Aldrich, #1185-53-1) pH 6.8, 1.5% (v/v) sodium dodecyl sulphate (SDS) (Gibco, #15553027), 10% (v/v) glycerol (Sigma-Aldrich, #56-81-5), 50 mM dithiothreitol (DTT) (Sigma-Aldrich, #D0632), protease inhibitor cocktail (Roche, #11697498001) and 25 U/mL benzonase (Sigma-Aldrich, #9025-65-4). Then, cells were scraped and collected. All lysates were stored at -80°C until the western blot was performed.

Before loading, 1 part of 4x Laemmli Sample Buffer (BioRad, #161-0747) containing 10% (v/v) β-mercaptoethanol (Sigma-Aldrich, #60-24-2) was added to 3 parts of all samples. Afterwards, samples were loaded on hand-cast polyacrylamide mini gels composed of a stacking gel containing 125 mM Tris-HCl pH 6.8, 4% (v/v) acrylamide:bisacrylamide (Bio-Rad, #1610154), 0.1% (v/v) glycerol (Sigma-Aldrich, #56-81-5), 0.1% (v/v) SDS (Gibco, #15553027), 0.075% (v/v) ammonium persulfate (APS) (Bio-Rad, #1610700), 0.17% (v/v) TEMED (Sigma, T9281) and of a resolving gel containing 375 mM Tris-HCl pH 8.8, 10% (v/v) acrylamide:bisacrylamide, 0.1% (v/v) glycerol, 0.1% (v/v) SDS, 0.075% (v/v) APS, 0.11% (v/v) TEMED. SDS-PAGE was performed in a 1x solution of 10x Tris-Glycine-SDS buffer (Bio-Rad, #161-0772) at 60-120V. Then, the PVDF transfer membrane (Thermo Scientific, #88518) was activated using methanol and proteins present in the resolving gel were wet-transferred to the membrane in a 1x solution of 10x Tris-Glycine buffer (Bio-Rad, #161-0771) at 400 mV for 90min. All membranes were blocked with a 5% (w/v) non-fat milk (Molico, Nestlé) solution, prepared in PBS containing 0.1% (v/v) Tween 20 (Biolife Italiana, #42120502) (PBS-T) for 1h. After blocking, membranes were incubated with 1:3000 dilution of Anti-CFTR (CFF, 596) and Anti-Calnexin (BD Transduction Laboratories, #610523) primary antibodies in 5% (w/v) non-fat milk in PBS-T, overnight at 4°C with constant agitation. Then, membranes were washed 3 times with PBS-T for 10 min each and incubated with Goat Anti-Mouse IgG (H + L)-HRP Conjugate Secondary Antibody (BioRad, #170-6516) for 1h at RT.

Membranes were imaged on the ChemiDoc XRS+ System (Bio-Rad, #170-8265) and the substrate solution for the chemiluminescent reaction was added. The substrate solution was prepared by mixing substrate luminol/enhancer with peroxide solution in a 1:1 ratio (Bio-Rad, #170-5061). Band intensity quantification was performed using the ImageLab software (Bio-Rad, #170-9690) and normalized to calnexin (loading control). The CFTR processing efficiency for each condition was assessed by dividing the quantified intensity of Band C by the total CFTR intensity (Band B+C) after normalization to the loading control.

### 3.4. Halide-Sensitive Yellow Fluorescent Protein (hsYFP) quenching assay

YFP is one of several Green Fluorescent Protein (GFP) derivatives. To increase EYFP (GFP - p.Ser65Gly/p.Val68Leu/p.Ser72Ala/p.Thr203Tyr) sensitivity to halides, like iodide and chloride, two additional mutations were added: histidine was replaced by glutamine at position 148 (p.His148Gln) and isoleucine by leucine at position 152 (p.Ile152Leu) by mutagenesis (EYFP p.His148Gln/p.Ile152Leu, hsYFP). (Pedemonte et al., 2011) The hsYFP stably expressed by the CFBE cells used in this work has an additional mutation, p.Phe46Leu, which accelerates chromophore oxidation at 37°C. (Zhong et al., 2014)

We performed a CFTR functional assay based on monitoring the hsYFP fluorescence quenching after iodide addition (Amaral et al., 2020; Sondo et al., 2011). CFBE cells co-expressing p.Phe508del-CFTR and hsYFP (18 500 cells/well) were seeded in 96-well imaging plates (Greiner, #655090) in MEM supplemented with 10% (v/v) FBS and after 24h were treated with CCG273441 (75nM, 100nM, 300nM, 500nM, 750nM and 1000nM) in MEM containing 1% FBS with VX-445 (3μM) and VX-661 (5μM). Wells with VX-661 and VX-445, and vehicle (0.05% DMSO) were used as controls. Cells were treated for 48h with media being replaced after 24 hours. At the time of the assay, cells were washed twice with PBS (137mM NaCl, 2.7mM KCl, 8.1mM $Na_2HPO_4$, 1.5mM $KH_2PO_4$) supplemented with 1mM $CaCl_2$, and 0.5mM $MgCl_2$ ($PBS^{+/+}$) pH 7.4, and incubated with $PBS^{+/+}$ containing forskolin (20μM) and VX-770 (3μM) for 30min at 37°C in the absence of $CO_2$ for CFTR stimulation. After incubation, fluorescence was measured with the Tecan Infinite F200 Pro plate reader for 2 sec before and 13 sec after iodide solution ($PBS^{+/+}$ with NaCl replaced by NaI) for a final $I^-$ concentration of 100mM in each well. Fluorescence values were normalized to the initial background-subtracted fluorescence (F/F0) and CFTR activity was measured by hsYFP quenching.

### 3.5. Statistical Analysis

To assess normality, the Shapiro-Wilk test was performed on all data. Statistical variation in Western blot experiments were assessed through normalization of all measurements for the control followed by One sample *t*-tests comparing the fold change variations versus the quantification baseline. For hsYFP assays, significance was assessed by one-way ANOVA followed by Dunnett's post hoc test. All data is presented as Mean ± SD. All statistical analyses were performed in the GraphPad Prism software version 9.0. Differences between test and control were considered statistically significant when the p-value was less than 0.05 ($p<0.05$). The number of independent biological replicates is indicated next to each experiment.

## 4. Results and Discussion

### 4.1. Validation of the CCG273463 stock

In a previous study developed in the host lab, CCG273463 was shown to rescue p.Phe508del-CFTR traffic in a manner additive to CFTR correctors (Figure 1.4.) (Amaral et al., 2023). Therefore, this inhibitor was initially chosen as a tool to investigate the traffic and regulation of CFTR as a function of the GRK5 activation status. To validate CCG273463 bioactivity, we examined its effect on CFTR expression and traffic by assessing p.Phe508del-CFTR levels through WB. CFTR can be detected in WB in its two forms: immature core-glycosylated form (known as band B) and mature fully glycosylated (known as band C). Due to the much stricter protein folding quality control mechanisms in the ER versus peripheral cellular compartments, the detection of band C is interpreted as a reporter of the functional CFTR pool. As presented in Figure 4.1., concentrations of CCG273463 above 300nM progressively increased core-glycosylated p.Phe508del-CFTR (band B) but not its fully-glycosylated form (band C).

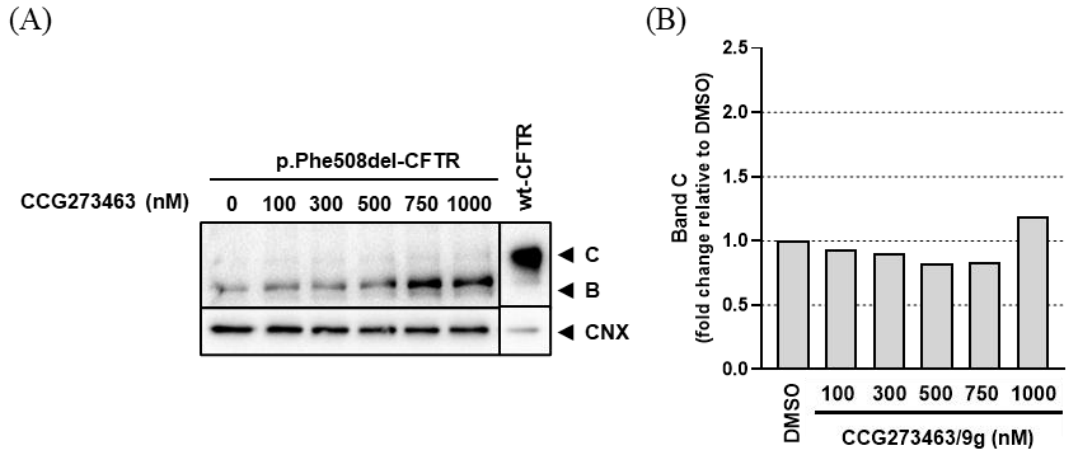


**Figure 4.1. CCG273463 effect on p.Phe508del-CFTR processing.** Detection of p.Phe508del-CFTR (Band B and C) and calnexin (CNX) expression (A) and quantification of p.Phe508del-CFTR band C (B) in CFBE cell lysates through western blotting. The p.Phe508del-CFTR CFBE cells were treated with vehicle (DMSO)and several CCG273463 concentrations for 24h. wt-CFTR CFBE cells were treated with vehicle for 24h and included as a reference of band B and C molecular weights.

The inefficacy in restoring band C, inconsistent with results previously obtained by our group, together with a high-resolution mass spectrometry analysis, of the CCG273463 stock which revealed ionic fragments not consistent with CCG273463 suggested a possible degradation of the compound (Figure 7.1.). We therefore disregarded the cellular responses in Figure 4.1.

## 4.2. CCG273441 effect on p.Phe508del-CFTR traffic in CFBE cell line

For this project, we were not able to obtain a fresh CCG273463 stock, after considering procurement from commercial sources and in-house synthesis by collaborators. To probe the effect of GRK5 activation in the regulation of CFTR traffic, we resorted to CCG273441, a structural analogue of CCG273463, with improved GRK5 IC50 (0.0038 ± 0.001μM) and similar selectivity (1:1300) (Table 1.1.), which we were able to obtain from a commercial source.

CCG273441 was used to study the effect of GRK5-inhibition in p.Phe508del-CFTR expression and traffic. Protein levels of p.Phe508del-CFTR were first assessed in CFBE cells treated with DMSO (vehicle), VX-661 and VX-445, and 6 different concentrations of CCG273441 for 24h and 48h. As presented in Figure 4.2., upon treatment with DMSO only the immature core-glycosylated CFTR (band B) can be observed reflecting p.Phe508del-CFTR impaired folding. When treated with the combination of VX-661 and VX-445 we identified a decrease in band B intensity and the emergence of a second band corresponding to 6.10-fold (24h treatment) and 8.24-fold (48h treatment) the fully-glycosylated CFTR (band C) present after treatment with DMSO, reflecting the folding corrective effect of these approved drugs. CCG273441 only presented a significant increase in CFTR expression and traffic when compared with DMSO after 48h of treatment. At this time point, CFTR band B levels increased significantly with CCG273441 at 75nM, 100nM and 300nM in 1.53-, 1.63- and 2.15-fold the band B with DMSO, respectively. These results show a positive effect of this GRK5 inhibitor in CFTR expression and/or stabilization (Figure 4.2.(C)). Contrarily, a significant decrease in CFTR band B was observed with 1000nM, revealing that CCG273441 has a concentration-dependent effect on CFTR expression. With 300nM CCG273441, the CFTR band C level also increased significantly, suggesting more CFTR was able to evade ER quality control (ERQC) (Figure 4.2.(B)). However, it corresponds to 1.53-fold the band C upon treatment with the vehicle, having little impact on the amount of mature p.Phe508del-CFTR. Regarding the processing efficiency, a significant decrease is observed with 300nM CCG273441, revealing that most p.Phe508del-CFTR is retained in the ER (Figure 4.2.(D)). Globally,

these results reveal that GRK5 inhibition with CCG273441 is more efficient in increasing p.Phe508del-CFTR expression/stability than its capacity to evade ERQC and traffic to the PM.

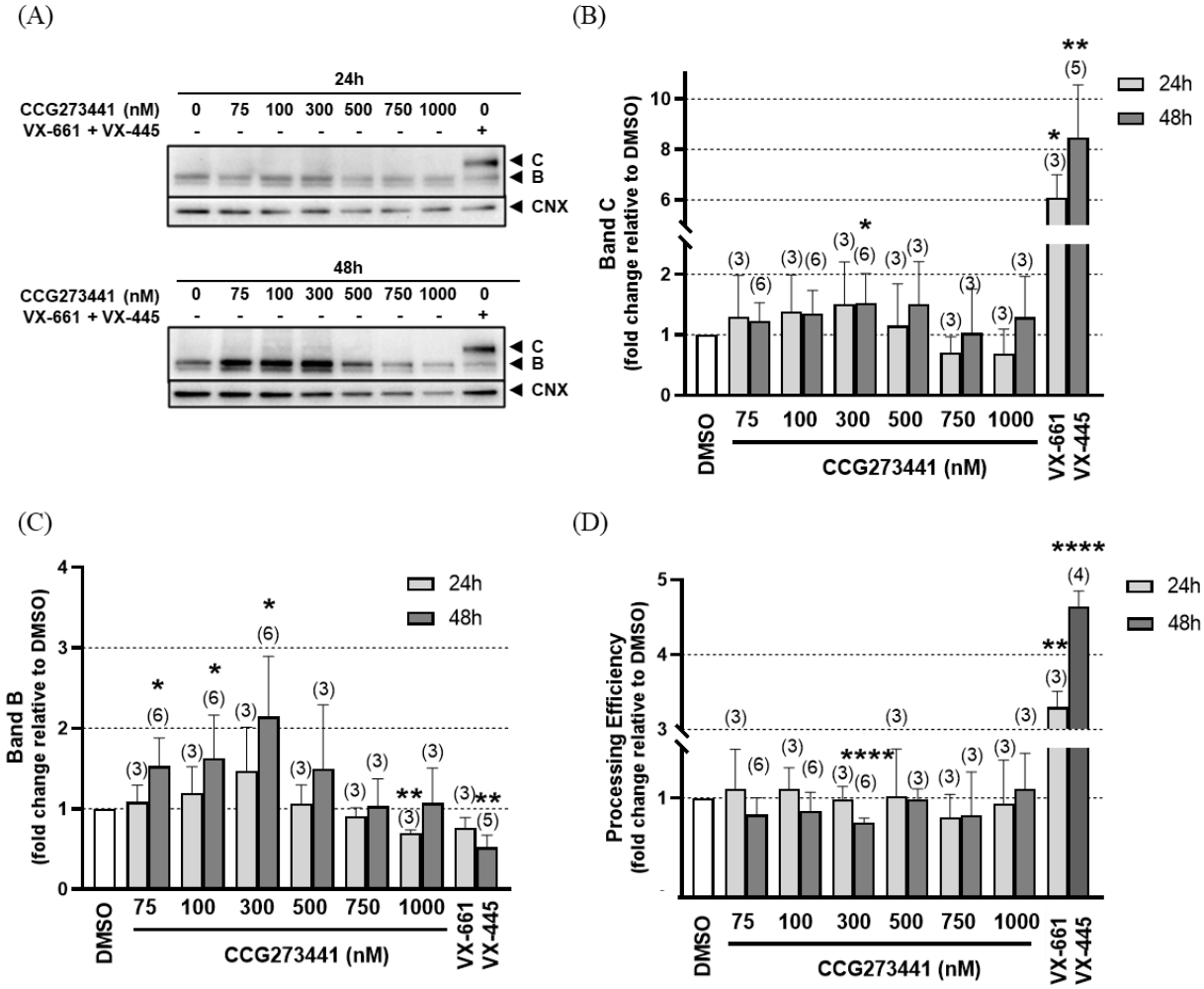


**Figure 4.2. CCG273441 effect on p.Phe508del-CFTR processing.** Detection of p.Phe508del-CFTR (Band B and C) and calnexin (CNX) expression in CFBE cell lysates through western blotting (A). Quantification of p.Phe508del-CFTR band C (B), band B (C) and processing efficiency (D) after treatment with vehicle (DMSO), VX-661 (5μM) and VX-445 (3μM), and several CCG273441 concentrations for 24h and 48h. Data were normalized to DMSO and are shown as means ± SD. The number of replicates (n) is represented above each bar. *, $p < 0.05$; **, $p < 0.01$; ****, $p < 0.0001$ (One sample *t*-test).

Then, to evaluate if CCG273441 is additive with the FDA-approved correctors VX-661 and VX-445, p.Phe508del-CFTR expression and processing in CFBE cells was analyzed upon treatment with DMSO and the double combination of VX-661 and VX-445 (controls) and with the same 6 concentrations of CCG273441 in combination with correctors. Cells were treated for 24h and 48h. As presented in Figure 4.3., the CCG273441, VX-661 and VX-445 combination significantly increases CFTR expression and traffic when compared with correctors after 48 hours of treatment. CFTR band B levels significantly increased with CCG273441 at 100nM and 300nM in 1.34- and 2.10-fold the CFTR band B upon treatment with VX-611 and VX-445 showing an additive effect in CFTR expression (Figure 4.3.(C)). With 300nM CCG273441, the CFTR band C level also increased significantly presenting an additive effect of CCG273441 to correctors in the amount of fully-glycosylated CFTR present in the cells, corresponding to an increase in 2.14-fold the band C upon treatment with correctors (Figure 4.3.(B)). Additionally, a significant decrease was observed in band B and band C when cells were treated with 75nM CCG273411 combined with VX-661 and VX-445, once again showing that CCG273441 has a concentration-dependent effect. Moreover, contrary to what was observed with

CCG273441 alone (Figure 4.2.(D)), the combination of CCG273441 with VX-661 and VX-445 showed no significant alteration in p.Phe508del-CFTR processing efficiency (Figure 4.3.(D)), which suggests that CCG273441 synergizes with CFTR folding correctors by enhancing the cellular CFTR pool without significantly improving folding efficiency.

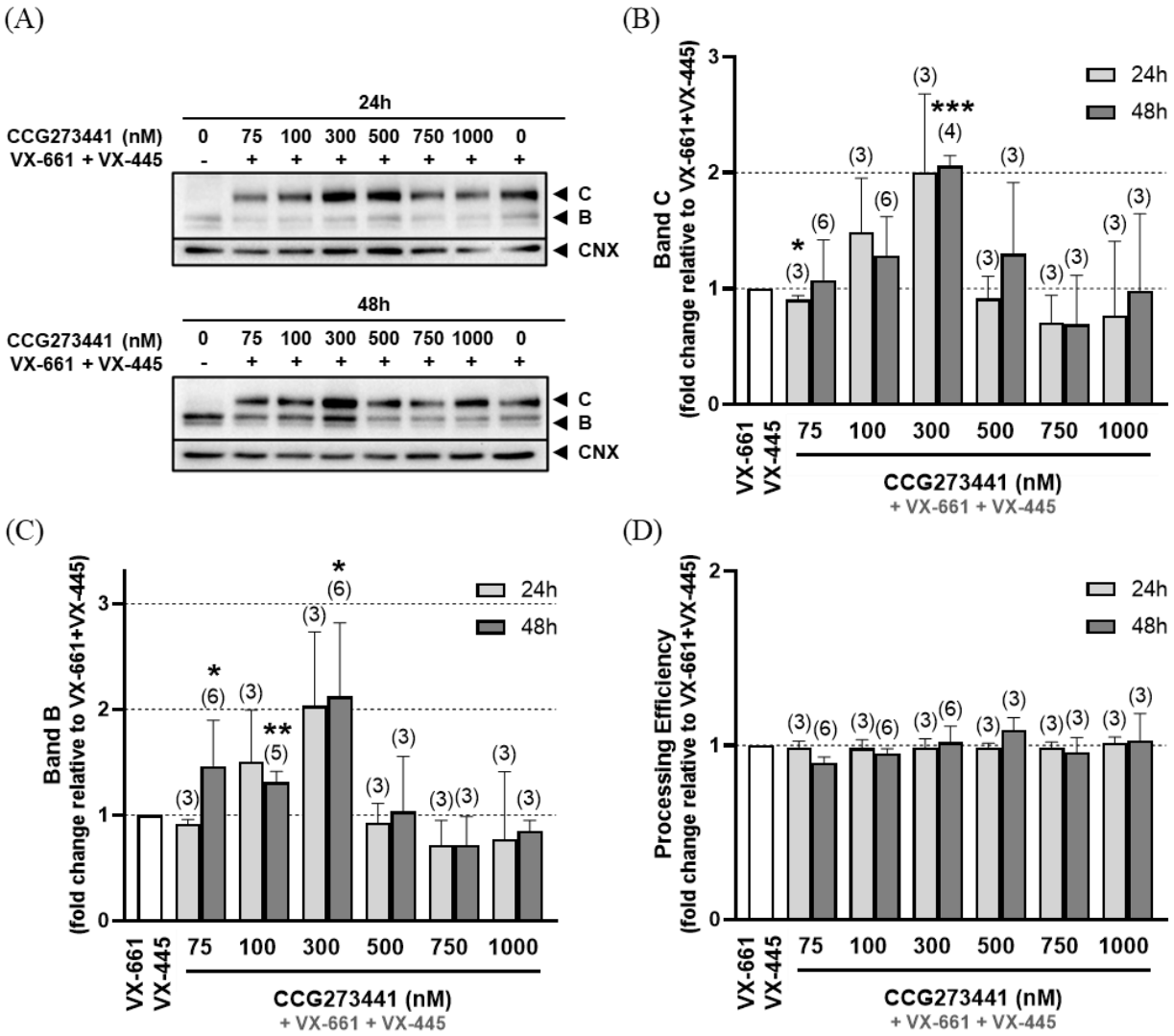


**Figure 4.3. Effect of the CCG273441, VX-661 and VX-445 combination on p.Phe508del-CFTR processing in CFBE cells.** Detection of p.Phe508del-CFTR (Band B and C) and calnexin (CNX) expression through western blotting (A). Quantification of p.Phe508del-CFTR band C (B), band B (C) and processing efficiency (D) after treatment with vehicle (DMSO), VX-661 (5µM) and VX-445 (3µM), and several CCG273441 concentrations plus VX-661 and VX-445 for 24h and 48h. Data were normalized to VX-661 + VX-445 and are shown as means ± SD. The number of replicates (n) is represented above each bar. *, $p < 0.05$; **, $p < 0.01$; ***, $p < 0.001$ (One sample *t*-test).

## 4.3. CCG273441 effect on p.Phe508del-CFTR traffic in 16HBE cell line

To assess if the additivity of CCG273441 with VX-661 and VX-445 is also observed in cells with endogenous expression of CFTR – *i.e.* at more physiologically relevant levels – we resorted to the 16HBE cell line. Protein levels of p.Phe508del-CFTR were assessed in 16HBE cells treated with DMSO and the double combination of VX-661 and VX-445 (controls), and with the same 6 concentrations of CCG273441 in combination with correctors, as performed with the CFBE cells. Cells were treated for 24h and 48h. In Figure 4.4., the CCG273441, VX-661 and VX-445 combination significantly increases

CFTR expression and traffic compared with correctors after 24 and 48 hours of treatment. CFTR band B levels increase significantly with CCG273441 at 75nM and 1000nM after 24h, and 300nM after 48h treatment. These results show an additive effect of CCG273441 to VX-611 and VX-445 resulting in increased core-glycosylated CFTR amount (Figure 4.4.(C)). CFTR band C levels increased significantly with CCG273441 at 75nM and 500nM after 24h, and 300nM after 48h treatment. Compared with band C upon treatment with correctors, CFTR band C increased 1.51- and 1.76-fold with 75nM and 500nM CCG273441 after 24h and 2.33-fold with 300nM after 48h (Figure 4.4.(B)). No significant alteration was observed in processing efficiency (Figure 4.4.(D)). Thus, it is possible to observe the additive effect of CCG273441, VX-661 and VX-445 in p.Phe508del-CFTR in two different cellular models.

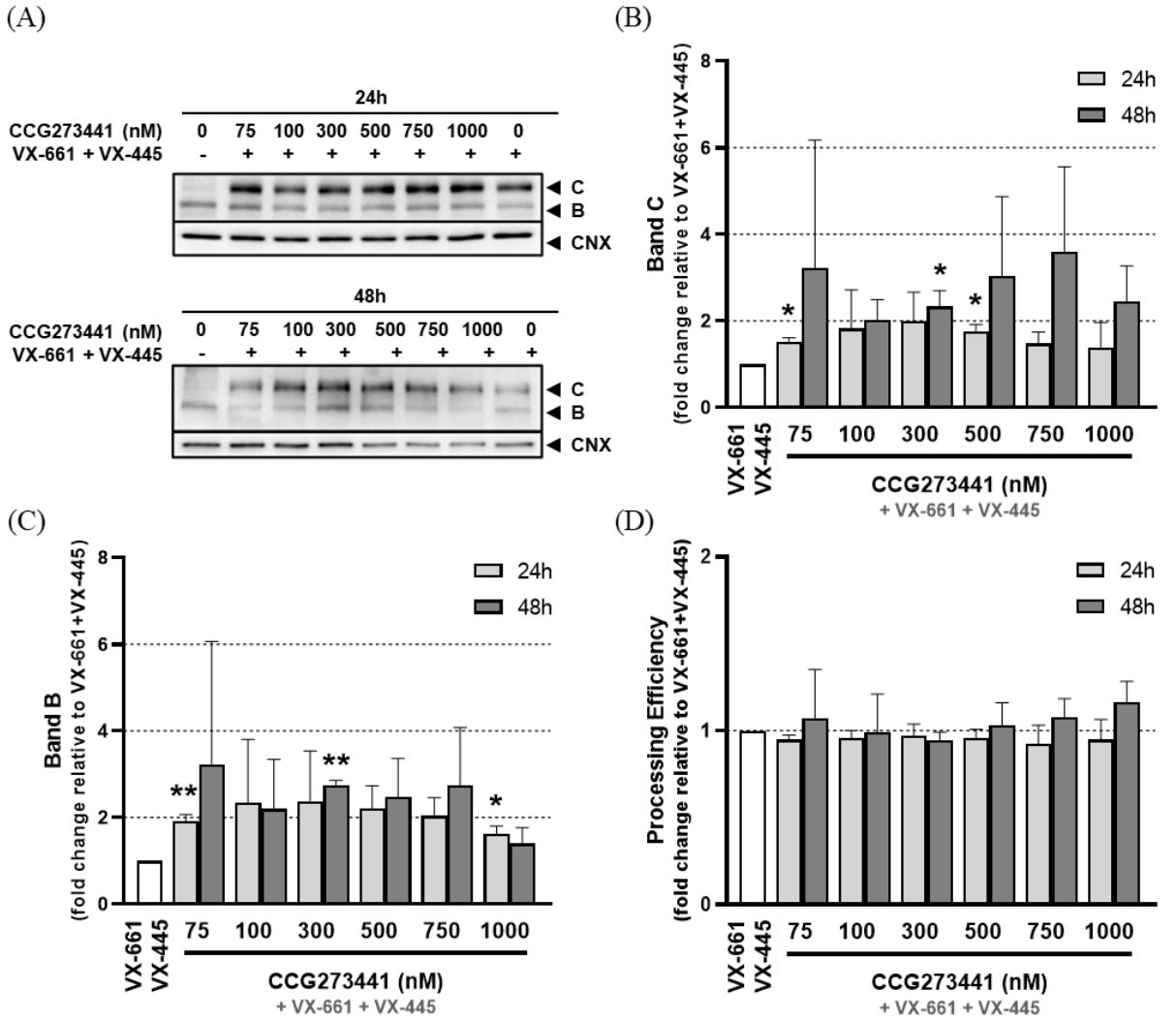


**Figure 4.4. Effect of the CCG273441, VX-661 and VX-445 combination on p.Phe508del-CFTR processing in 16HBE cells.** Detection of p.Phe508del-CFTR (Band B and C) and calnexin (CNX) expression through western blotting (A). Quantification of p.Phe508del-CFTR band C (B), band B (C) and processing efficiency (D) after treatment with vehicle (DMSO), VX-661 (5µM) and VX-445 (3µM), and several CCG273441 concentrations plus VX-661 and VX-445. Data were normalized to VX-661 + VX-445 and are shown as means ± SD, n=3. *, $p < 0.05$; **, $p < 0.01$ (One sample *t*-test).

## 4.4. CCG273441 impact on p.Phe508del-CFTR function in CFBE cell line

Subsequently, the effect of the CCG273441, VX-661 and VX-445 combination on p.Phe508del-CFTR function was evaluated by assessing the hsYFP fluorescence quenching rate after 48h of treatment with DMSO and the double combination of VX-661 and VX-445 (controls), and the same CCG273441 concentrations used in the WB. In this 96 wellplate-based assay, CFTR activity is quantitated by adding

iodide to cells co-expressing hsYFP and p.Phe508del-CFTR. In the presence of CFTR agonists, permeation of iodide ions through CFTR results in mono-exponential YFP quenching, whose rate constant is proportional to CFTR activity. In our experiments, CFTR activity is reported as the quenching curve derivative at the instant of iodide addition. The results reveal a similar hsYFP quenching curve and fit when cells were treated with VX-661 plus VX-445 alone and in combination with 75nM and 100nM CCG273441 (Figure 4.5.(A)) and consequently similar CFTR activity (Figure 4.5.(B)). When treated with 300nM, 500nM, 750nM and 1000nM, combined with VX-661 and VX-445, the quenching rate is visibly higher when compared with VX-661 and VX-445 alone (Figure 4.5.(A)), reflecting a significant increase in CFTR activity (Figure 4.5.(B)). However, it is known that toxic compound concentrations lead to cell detachment when iodide solution is injected, resulting in a sharp fluorescence drop that may be confused with increased CFTR activity. (Pedemonte et al., 2011) This limitation may justify the apparent high CFTR function with 750nM and 1000nM CCG273441 (Figure 4.5.), concentrations that do not increase fully-glycosylated CFTR (Figure 4.3.(B)).

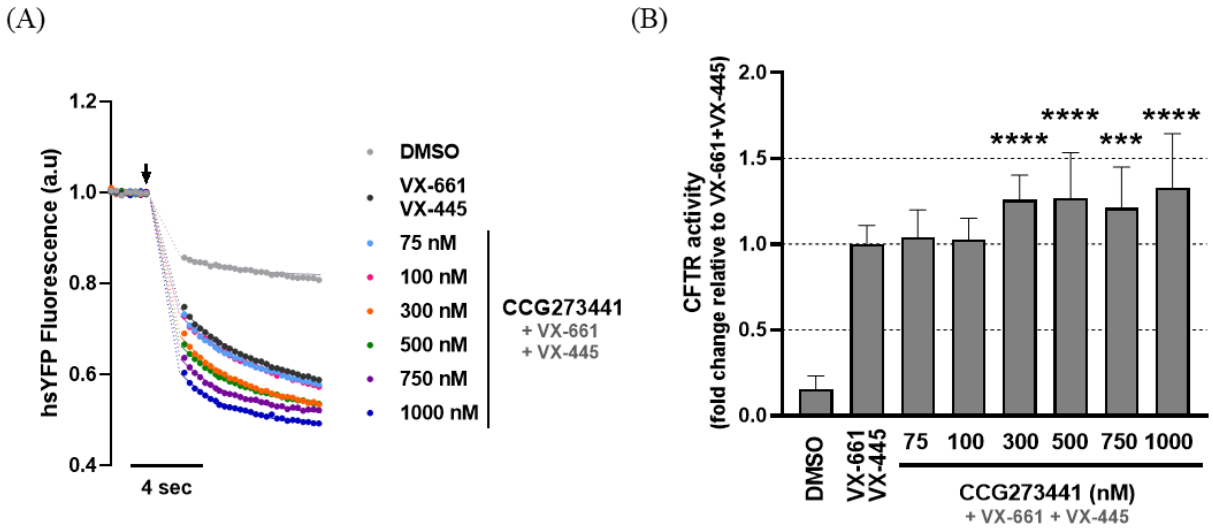


**Figure 4.5. Effect of the CCG273441, VX-661 and VX-445 combination on p.Phe508del-CFTR channel activity.** (A) Representative hsYFP-quenching curves and fit obtained upon $I^-$ (100mM) addition in CFBE p.Phe508del-CFTR cells co-expressing hsYFP after 48h treatment with DMSO, VX-661 (5μM) and VX-445 (3μM) alone and in combination with several concentrations of CCG273441. The arrow indicates iodide addition. Dashed lines were added to guide the eye during the 2-second long gap when iodide is added. (B) CFTR activity quantification based on the hsYFP quenching rate and normalized to VX-661 and VX-445 combination. Data are represented as Mean ± SD, n=4. ***, $p < 0.001$; ****, $p < 0.0001$ (One-way ANOVA).

To investigate the potential CCG273441 toxicity in the hsYFP assay, we analyzed the initial baseline YFP fluorescence in each experimental condition, in a manner inspired by classical fluorescence-based cytotoxicity assays (Kalinina et al., 2018). As observed in Figure 4.6., there is a decrease in hsYFP initial fluorescence when cells are treated with CCG273441 concentrations above 100nM, suggesting a drop of cell viability to 83.8% at 300nM, 74.8% at 500nM, 62% at 750nM and 53.8% at 1000nM, indicating CCG273441 toxicity 750nM and 1000nM.

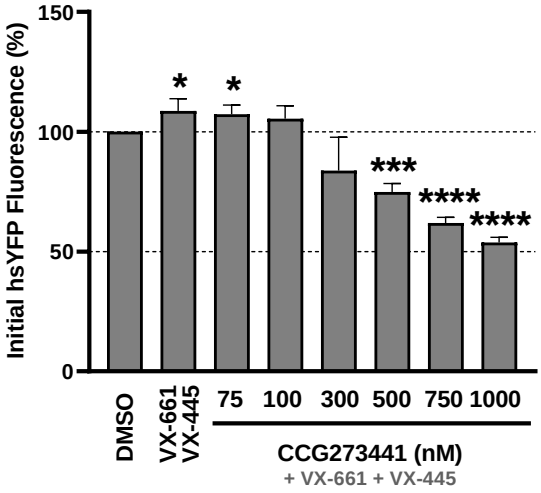


**Figure 4.6. Initial hsYFP Fluorescence**. CFBE p.Phe508del-CFTR cells exposed to DMSO, VX-661 (5μM) and VX-445 (3μM) combination alone and with different concentrations of CCG273441. Data are represented as Mean ± SD, n=4. *, $p < 0.05$, ***, $p < 0.001$; ****, $p < 0.0001$ (One sample *t*-test).

At the functional level, our results indicate that in the CFBE cell model expressing p.Phe508del-CFTR, CCG273441 is additive to the VX-661 plus VX-445 corrector combination in rescuing CFTR activity. Our results also suggest that the useful CCG273441 concentration range is quite narrow (around 300nM), due to cytotoxicity above 100nM. At 300 nM we observed statistically significant additivity with the clinical modulator combination on p.Phe508del-CFTR functional rescue in the hsYFP assay, while keeping high cell viability. These data also indicate that these conditions may be used in further experiments to dissect the mechanism of action of CCG273441 in terms of p.Phe508del-CFTR rescue.

# 5. Conclusion and Future perspectives

Globally, our results confirmed that GRK5 plays a role in p.Phe508del-CFTR regulation, with this effect being observed in two different bronchial cell lines, CFBE and 16HBE. GRK5 regulates p.Phe508del-CFTR through a different mechanism than CFTR modulators. This kinase seems to interfere with CFTR production and/or degradation, increasing the pool p.Phe508del-CFTR and thus the amount prone to be corrected by the CFTR modulators.

In CFBE cells, the GRK5 inhibition alone showed a major impact in increasing the amount of immature core glycosylated CFTR rather than mature fully glycosylated CFTR, an effect altered when CCG273441 was combined with the approved CFTR modulators VX-661 and VX-445. When cells were treated with this combination of compounds containing 300nM CCG273441 for 48h, the amount of core-glycosylated p.Phe508del-CFTR was similar to when CCG273441 was used alone while fully glycosylated p.Phe508del-CFTR increased from a statistically non-significant 1.53-fold relative to DMSO to 2.14-fold relative to VX-661 and VX-445, which has a band C of 8.24-fold relative to DMSO. Thus, this drug combination is estimated to increase in around 18-fold the amount of fully glycosylated CFTR present in untreated p.Phe508del-CFTR CFBE cells. In 16HBE cells, the fully glycosylated p.Phe508del-CFTR increased 2.33-fold relative to VX-661 and VX-445 after treatment with 300nM CCG273441 combined with modulators for 48h.

The hsYFP quenching assay confirmed that the GRK5 inhibition effect on the expression and/or stabilization of p.Phe508del-CFTR followed by modulators-mediated folding correction resulted in increased functional p.Phe508del-CFTR at the PM with 83.8% cell viability.

Further investigation of the GRK5-CFTR signalling pathway composition would help to elucidate how GRK5 regulates p.Phe508del-CFTR. Some useful approaches to highlight this pathway could be

the identification of GRK5 interactors through immunoprecipitation-based SWATH proteomics, followed by validation through high-content siRNA screenings (Botelho et al., 2015) to identify genes whose expression is required for the CCG273441 additivity phenotype on CFTR PM expression. Additionally, the intervention of second messengers, other small molecules or metabolic enzymes can be investigated through a differential metabolomics analysis of cells in control or CCG273441-treated conditions.

# 6. References


Allan, K. M., Farrow, N., Donnelley, M., Jaffe, A., & Waters, S. A. (2021). Treatment of Cystic Fibrosis: From Gene- to Cell-Based Therapies. *Frontiers in Pharmacology*, *12*, 639475. https://doi.org/10.3389/fphar.2021.639475

Amaral, M. D. (2005). Processing of CFTR: Traversing the cellular maze—How much CFTR needs to go through to avoid cystic fibrosis? *Pediatric Pulmonology*, *39*(6), 479–491. https://doi.org/10.1002/ppul.20168

Amaral, M. D. (2015). Novel personalized therapies for cystic fibrosis: Treating the basic defect in all patients. *Journal of Internal Medicine*, *277*(2), 155–166. https://doi.org/10.1111/joim.12314

Amaral, M. D., Botelho, H. M., & Lopes-Pacheco, M. (2023). *Method of identifying agents for the treatment of cystic fibrosis caused by the mutation F508del.* (WIPO Patent PCT/IB2023/051813).

Amaral, M. D., Hutt, D. M., Tomati, V., Botelho, H. M., & Pedemonte, N. (2020). CFTR processing, trafficking and interactions. *Journal of Cystic Fibrosis*, *19*, S33–S36. https://doi.org/10.1016/j.jcf.2019.10.017

Andersen, D. H. (1938). CYSTIC FIBROSIS OF THE PANCREAS AND ITS RELATION TO CELIAC DISEASE: A CLINICAL AND PATHOLOGIC STUDY. *American Journal of Diseases of Children*, *56*(2), 344. https://doi.org/10.1001/archpedi.1938.01980140114013

Andersen, D. H. (1946). CELIAC SYNDROME: V. Genetics of Cystic Fibrosis of the Pancreas With a Consideration of Etiology. *American Journal of Diseases of Children*, *72*(1), 62. https://doi.org/10.1001/archpedi.1946.02020300069004

Bacalhau, M., Camargo, M., Magalhães-Ghiotto, G. A. V., Drumond, S., Castelletti, C. H. M., & Lopes-Pacheco, M. (2023). Elexacaftor-Tezacaftor-Ivacaftor: A Life-Changing Triple Combination of CFTR Modulator Drugs for Cystic Fibrosis. *Pharmaceuticals*, *16*(3), 410. https://doi.org/10.3390/ph16030410

Bose, S. J., Krainer, G., Ng, D. R. S., Schenkel, M., Shishido, H., Yoon, J. S., Haggie, P. M., Schlierf, M., Sheppard, D. N., & Skach, W. R. (2020). Towards next generation therapies for cystic fibrosis: Folding, function and pharmacology of CFTR. *Journal of Cystic Fibrosis*, *19*, S25–S32. https://doi.org/10.1016/j.jcf.2019.12.009

Botelho, H. M., Uliyakina, I., Awatade, N. T., Proença, M. C., Tischer, C., Sirianant, L., Kunzelmann, K., Pepperkok, R., & Amaral, M. D. (2015). Protein Traffic Disorders: An Effective High-Throughput Fluorescence Microscopy Pipeline for Drug Discovery. *Scientific Reports*, *5*(1), 9038. https://doi.org/10.1038/srep09038

Brown, S. D., White, R., & Tobin, P. (2017). Keep them breathing: Cystic fibrosis pathophysiology, diagnosis, and treatment. *JAAPA*, *30*(5), 23–27. https://doi.org/10.1097/01.JAA.0000515540.36581.92

Capurro, V., Tomati, V., Sondo, E., Renda, M., Borrelli, A., Pastorino, C., Guidone, D., Venturini, A., Giraudo, A., Mandrup Bertozzi, S., Musante, I., Bertozzi, F., Bandiera, T., Zara, F., Galietta, L. J. V., & Pedemonte, N. (2021). Partial Rescue of F508del-CFTR Stability and Trafficking Defects by Double Corrector Treatment. *International Journal of Molecular Sciences*, *22*(10), 5262. https://doi.org/10.3390/ijms22105262

Chen, Y., Sonawane, A., Manda, R., Gadi, R. K., Tesmer, J. J. G., & Ghosh, A. K. (2024). Development of a new class of potent and highly selective G protein-coupled receptor kinase 5 inhibitors and structural insight from crystal structures of inhibitor complexes. *European Journal of Medicinal Chemistry*, *264*, 115931. https://doi.org/10.1016/j.ejmech.2023.115931

Coverstone, A. M., & Ferkol, T. W. (2021). Early Diagnosis and Intervention in Cystic Fibrosis: Imagining the Unimaginable. *Frontiers in Pediatrics*, *8*, 608821. https://doi.org/10.3389/fped.2020.608821

Cromwell, E. A., Ostrenga, J. S., Todd, J. V., Elbert, A., Brown, A. W., Faro, A., Goss, C. H., & Marshall, B. C. (2023). Cystic fibrosis prevalence in the United States and participation in the Cystic Fibrosis Foundation Patient Registry in 2020. *Journal of Cystic Fibrosis*, *22*(3), 436–442. https://doi.org/10.1016/j.jcf.2023.02.009

De Boeck, K., & Amaral, M. D. (2016). Progress in therapies for cystic fibrosis. *The Lancet Respiratory Medicine*, *4*(8), 662–674. https://doi.org/10.1016/S2213-2600(16)00023-0

Dekkers, J. F., Wiegerinck, C. L., De Jonge, H. R., Bronsveld, I., Janssens, H. M., De Winter-de Groot, K. M., Brandsma, A. M., De Jong, N. W. M., Bijvelds, M. J. C., Scholte, B. J., Nieuwenhuis, E. E. S., Van Den Brink, S., Clevers, H., Van Der Ent, C. K., Middendorp, S., & Beekman, J. M. (2013). A functional CFTR assay using primary cystic fibrosis intestinal organoids. *Nature Medicine*, *19*(7), 939–945. https://doi.org/10.1038/nm.3201

Elborn, J. S. (2016). Cystic fibrosis. *The Lancet*, *388*(10059), 2519–2531. https://doi.org/10.1016/S0140-6736(16)00576-6

Fajac, I., & Sermet, I. (2021). Therapeutic Approaches for Patients with Cystic Fibrosis Not Eligible for Current CFTR Modulators. *Cells*, *10*(10), 2793. https://doi.org/10.3390/cells10102793

Farinha, C. M., & Callebaut, I. (2022). Molecular mechanisms of cystic fibrosis – how mutations lead to misfunction and guide therapy. *Bioscience Reports*, *42*(7), BSR20212006. https://doi.org/10.1042/BSR20212006

Farinha, C. M., & Canato, S. (2017). From the endoplasmic reticulum to the plasma membrane: Mechanisms of CFTR folding and trafficking. *Cellular and Molecular Life Sciences*, *74*(1), 39–55. https://doi.org/10.1007/s00018-016-2387-7

Girón Moreno, R. M., García-Clemente, M., Diab-Cáceres, L., Martínez-Vergara, A., Martínez-García, M. Á., & Gómez-Punter, R. M. (2021). Treatment of Pulmonary Disease of Cystic Fibrosis: A Comprehensive Review. *Antibiotics*, *10*(5), 486. https://doi.org/10.3390/antibiotics10050486

Gottschalk, L. B., Vecchio-Pagan, B., Sharma, N., Han, S. T., Franca, A., Wohler, E. S., Batista, D. A. S., Goff, L. A., & Cutting, G. R. (2016). Creation and characterization of an airway epithelial cell line for stable expression of CFTR variants. *Journal of Cystic Fibrosis*, *15*(3), 285–294. https://doi.org/10.1016/j.jcf.2015.11.010

Guo, J., Garratt, A., & Hill, A. (2022). Worldwide rates of diagnosis and effective treatment for cystic fibrosis. *Journal of Cystic Fibrosis*, *21*(3), 456–462. https://doi.org/10.1016/j.jcf.2022.01.009

Heijerman, H. G. M., McKone, E. F., Downey, D. G., Van Braeckel, E., Rowe, S. M., Tullis, E., Mall, M. A., Welter, J. J., Ramsey, B. W., McKee, C. M., Marigowda, G., Moskowitz, S. M., Waltz, D., Sosnay, P. R., Simard, C., Ahluwalia, N., Xuan, F., Zhang, Y., Taylor-Cousar, J. L., … Majoor, C.

(2019). Efficacy and safety of the elexacaftor plus tezacaftor plus ivacaftor combination regimen in people with cystic fibrosis homozygous for the F508del mutation: A double-blind, randomised, phase 3 trial. *The Lancet*, *394*(10212), 1940–1948. https://doi.org/10.1016/S0140-6736(19)32597-8

Hendrickx, J. O., Van Gastel, J., Leysen, H., Santos-Otte, P., Premont, R. T., Martin, B., & Maudsley, S. (2018). GRK5 – A Functional Bridge Between Cardiovascular and Neurodegenerative Disorders. *Frontiers in Pharmacology*, *9*, 1484. https://doi.org/10.3389/fphar.2018.01484

Hwang, T.-C., Yeh, J.-T., Zhang, J., Yu, Y.-C., Yeh, H.-I., & Destefano, S. (2018). Structural mechanisms of CFTR function and dysfunction. *Journal of General Physiology*, *150*(4), 539–570. https://doi.org/10.1085/jgp.201711946

Kalinina, M. A., Skvortsov, D. A., Rubtsova, M. P., Komarova, E. S., & Dontsova, O. A. (2018). Cytotoxicity Test Based on Human Cells Labeled with Fluorescent Proteins: Fluorimetry, Photography, and Scanning for High-Throughput Assay. *Molecular Imaging and Biology*, *20*(3), 368–377. https://doi.org/10.1007/s11307-017-1152-0

Liu, F., Zhang, Z., Csanády, L., Gadsby, D. C., & Chen, J. (2017). Molecular Structure of the Human CFTR Ion Channel. *Cell*, *169*(1), 85-95.e8. https://doi.org/10.1016/j.cell.2017.02.024

Lopes-Pacheco, M. (2020). CFTR Modulators: The Changing Face of Cystic Fibrosis in the Era of Precision Medicine. *Frontiers in Pharmacology*, *10*, 1662. https://doi.org/10.3389/fphar.2019.01662

Meng, X., Clews, J., Kargas, V., Wang, X., & Ford, R. C. (2017). The cystic fibrosis transmembrane conductance regulator (CFTR) and its stability. *Cellular and Molecular Life Sciences*, *74*(1), 23–38. https://doi.org/10.1007/s00018-016-2386-8

Middleton, P. G., Mall, M. A., Dřevínek, P., Lands, L. C., McKone, E. F., Polineni, D., Ramsey, B. W., Taylor-Cousar, J. L., Tullis, E., Vermeulen, F., Marigowda, G., McKee, C. M., Moskowitz, S. M., Nair, N., Savage, J., Simard, C., Tian, S., Waltz, D., Xuan, F., … Jain, R. (2019). Elexacaftor–Tezacaftor–Ivacaftor for Cystic Fibrosis with a Single Phe508del Allele. *New England Journal of Medicine*, *381*(19), 1809–1819. https://doi.org/10.1056/NEJMoa1908639

Moniz, S., Sousa, M., Moraes, B. J., Mendes, A. I., Palma, M., Barreto, C., Fragata, J. I., Amaral, M. D., & Matos, P. (2013). HGF Stimulation of Rac1 Signaling Enhances Pharmacological Correction of the Most Prevalent Cystic Fibrosis Mutant F508del-CFTR. *ACS Chemical Biology*, *8*(2), 432–442. https://doi.org/10.1021/cb300484r

Moran, O. (2017). The gating of the CFTR channel. *Cellular and Molecular Life Sciences*, *74*(1), 85–92. https://doi.org/10.1007/s00018-016-2390-z

Parisi, G. F., Mòllica, F., Giallongo, A., Papale, M., Manti, S., & Leonardi, S. (2022). Cystic fibrosis transmembrane conductance regulator (CFTR): Beyond cystic fibrosis. *Egyptian Journal of Medical Human Genetics*, *23*(1). https://doi.org/10.1186/s43042-022-00308-7

Pedemonte, N., Zegarra-Moran, O., & Galietta, L. J. V. (2011). High-Throughput Screening of Libraries of Compounds to Identify CFTR Modulators. In M. D. Amaral & K. Kunzelmann (Eds.), *Cystic Fibrosis* (Vol. 741, pp. 13–21). Humana Press. https://doi.org/10.1007/978-1-61779-117-8_2

Pfleger, J., Gresham, K., & Koch, W. J. (2019). G protein-coupled receptor kinases as therapeutic targets in the heart. *Nature Reviews Cardiology*, *16*(10), 612–622. https://doi.org/10.1038/s41569-019-0220-3

Railean, V., Rodrigues, C. S., Ramalho, S. S., Silva, I. A. L., Bartosch, J., Farinha, C. M., Pankonien, I., & Amaral, M. D. (2023). Personalized medicine: Function of CFTR variant p.Arg334Trp is rescued by currently available CFTR modulators. *Frontiers in Molecular Biosciences*, *10*, 1155705. https://doi.org/10.3389/fmolb.2023.1155705

Riordan, J. R., Rommens, J. M., Kerem, B.-S., Alon, N., Rozmahel, R., Grzelczak, Z., Zielenski, J., Lok, S., Plavsic, N., Chou, J.-L., Drumm, M. L., & Iannuzzi, M. C. (1989). Identification of the Cystic Fibrosis Gene: Cloning and Characterization of Complementary DNA. *Science*, *245*, 1066–1073. https://doi.org/10.1126/science.2475911

Roda, J., Pinto-Silva, C., Silva, I. A. I., Maia, C., Almeida, S., Ferreira, R., & Oliveira, G. (2022). New drugs in cystic fibrosis: What has changed in the last decade? *Therapeutic Advances in Chronic Disease*, *13*, 204062232210981. https://doi.org/10.1177/20406223221098136

Rowlands, R. A., Chen, Q., Bouley, R. A., Avramova, L. V., Tesmer, J. J. G., & White, A. D. (2021). Generation of Highly Selective, Potent, and Covalent G Protein-Coupled Receptor Kinase 5 Inhibitors. *Journal of Medicinal Chemistry*, *64*(1), 566–585. https://doi.org/10.1021/acs.jmedchem.0c01522

Scotet, V., L'Hostis, C., & Férec, C. (2020). The Changing Epidemiology of Cystic Fibrosis: Incidence, Survival and Impact of the CFTR Gene Discovery. *Genes*, *11*(6), 589. https://doi.org/10.3390/genes11060589

Shteinberg, M., Haq, I. J., Polineni, D., & Davies, J. C. (2021). Cystic fibrosis. *The Lancet*, *397*(10290), 2195–2211. https://doi.org/10.1016/S0140-6736(20)32542-3

Silva, I. A. L., Laselva, O., & Lopes-Pacheco, M. (2022). Advances in Preclinical In Vitro Models for the Translation of Precision Medicine for Cystic Fibrosis. *Journal of Personalized Medicine*, *12*(8), 1321. https://doi.org/10.3390/jpm12081321

Sondo, E., Tomati, V., Caci, E., Esposito, A. I., Pfeffer, U., Pedemonte, N., & Galietta, L. J. V. (2011). Rescue of the mutant CFTR chloride channel by pharmacological correctors and low temperature analyzed by gene expression profiling. *American Journal of Physiology-Cell Physiology*, *301*(4), C872–C885. https://doi.org/10.1152/ajpcell.00507.2010

Tsui, L.-C., & Dorfman, R. (2013). The Cystic Fibrosis Gene: A Molecular Genetic Perspective. *Cold Spring Harbor Perspectives in Medicine*, *3*(2), a009472–a009472. https://doi.org/10.1101/cshperspect.a009472

Van Den Bossche, S., Ostyn, L., Vandendriessche, V., Rigauts, C., De Keersmaecker, H., Nickerson, C. A., & Crabbé, A. (2023). The development and characterization of in vivo-like three-dimensional models of bronchial epithelial cell lines. *European Journal of Pharmaceutical Sciences*, *190*, 106567. https://doi.org/10.1016/j.ejps.2023.106567

Zajac, M., Dreano, E., Edwards, A., Planelles, G., & Sermet-Gaudelus, I. (2021). Airway Surface Liquid pH Regulation in Airway Epithelium Current Understandings and Gaps in Knowledge. *International Journal of Molecular Sciences*, *22*(7), 3384. https://doi.org/10.3390/ijms22073384

Zhong, S., Navaratnam, D., & Santos-Sacchi, J. (2014). A Genetically-Encoded YFP Sensor with Enhanced Chloride Sensitivity, Photostability and Reduced pH Interference Demonstrates Augmented Transmembrane Chloride Movement by Gerbil Prestin (SLC26a5). *PLoS ONE*, *9*(6), e99095. https://doi.org/10.1371/journal.pone.0099095

# 7. Supplementary Materials

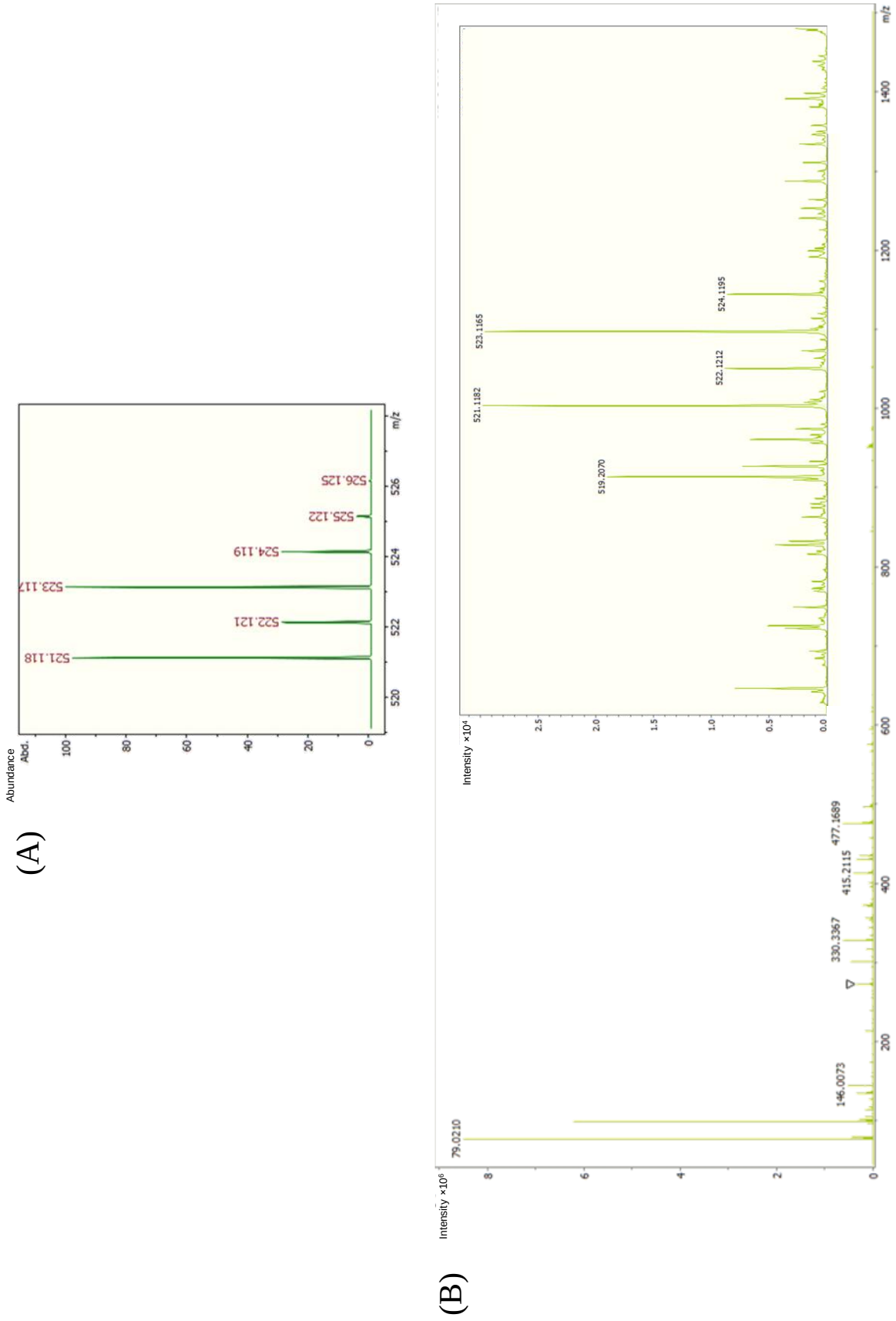


**Figure 7.1. Mass spectra of the CCG273463 stock solution.** (A) Predicted mass spectrum. (B) Experimental mass spectrum (inset showing ionic peaks associated with CCG273463).